STUDENT POSTERS

NUCLEAR DAYS 2024

Pilsen, Czech Republic

www.jadernedny.cz

Poster Scientific Committee

doc. Ing. František HEZOUČKÝ, Ph.D.	University of West Bohemia
Ing. Karel BÍŽA	ÚJV Řež, a. s.
Ing. Josef Královec, CS.	

Organizing Committee

Ing. Jan ZDEBOR, CSc.	University of West Bohemia
Ing. Michal VOLF	University of West Bohemia
Ing. Jana JIŘIČKOVÁ, Ph.D.	University of West Bohemia
Ing. David Mašata	University of West Bohemia
Ing. Jan Ullmann	University of West Bohemia
Ing. Eva Kozáková Krauzová	University of West Bohemia
Dr. Ing. Jaroslav Synáč	University of West Bohemia
Bc. Petr Vastl	University of West Bohemia
Bc. Tomáš Kadavý	University of West Bohemia
Bc. Anna Mrázová	University of West Bohemia
Bc. Lucie GRUSOVÁ	ŠKODA JS a.s.

Partners of Nuclear Days 2024

General partner

Platinum partner

Gold partners

Silver partners

Other partners

Media partners

Podpořeno

This event has been partially supported by the ENEN2plus project founded by the European Union (HORIZON-EURATOM- 2021-NRT-01-13 101061677).

BACHELOR STUDENTS

NUCLEAR POWER PLANTS IN DISTRICT HEAT

Tomáš Babický

Faculty of Electrical Engineering, University of West Bohemia, Czech Republic

The work addresses the issue of utilizing nuclear power plants in district heating in the Czech Republic. The main focus is on the Temelín Nuclear Power Plant, which has long been supplying heat to Týn nad Vltavou and, since 2023, also to České Budějovice. It specifically concentrates on the impact of the Temelín hot water pipeline on the district heating network in České Budějovice.

Nuclear power plants in district heating

FACULTY OF ELECTRICAL ENGINEERING
UNIVERSITY OF WEST BOHEMIA

Author: Bc. Tomáš Babický Supervisor: Ing. David Mašata

Introduction

The use of nuclear power plants in district heating is a crucial factor in achieving a carbon-neutral Europe. Cities heated by nuclear power plants can reduce heat production from conventional heating plants, boiler houses, and incineration facilities, thereby saving emissions from coal and natural gas. The aim of this study was to analyze the district heating systems of the Temelín and Dukovany nuclear power plants located in the Czech Republic.

Hot water pipeline from ETE to České Budějovice

- Costs: 2.4 billion CZK (investor ČEZ)
- Construction completion: 2023
- Pipeline length: 2 x 26 km
- Elevation gain: 120 m
- Outer diameter of pipes: 80 and 71 cm
- 2 suspended bridges; otherwise, 1.3 m underground
- Temperature of supplied water: 90 – 140 °C
- Heat supply losses: up to 3%
- Planned annual heat supply: 750 TJ
- Annual CO2 emissions savings: 80,000 tons
- Coverage of heat demand by the hot water pipeline in ČB: 30%
- Heat supply for 3 months of operation in 2023: 258 TJ
- Daily maximum heat supply to ČB: 5.6 TJ
- Heat price in 2023: 789 CZK / GJ

Heating of Týn nad Vltavou

- ETE (Temelín Nuclear Power Plant) has been heating Týn nad Vltavou since 1998
- Distance from ETE: 5 km
- Decommissioned: 22 heating plants and 3 large boilers
- Heat supplied in 2022: 183,000 GJ
- 470 houses and 2,100 apartments
- CO2 emissions reduction: 15,000 tons per year

Hot Water Pipeline from EDU (Dukovany Nuclear Power Plant) to Brno

- Expected launch: 2030
- Length: 42 km
- Coverage of heat demand in Brno: 50%
- Estimated cost: 19 billion CZK
- Annual estimated heat supply: 2,000 TJ
- Current heat price in Brno: 1,200 CZK / GJ
- Predicted heat price in Brno in 2030: 1,000 CZK / GJ

Calculations of Savings

- Savings of coal in ČB heating plant: 73,320,000 CZK
- Savings on unpurchased emission allowances: 147,920,000 CZK
- Comparison of heat prices from a heating plant and a nuclear power plant:
  - Selling price of heat energy from coal: 600 CZK / GJ
  - Theoretical price of heat energy from a nuclear power plant: 47.5 CZK / GJ
- Annual turnover of the ČB heating plant (2022): 1,150,331,000 CZK

Development of heat production in Brno

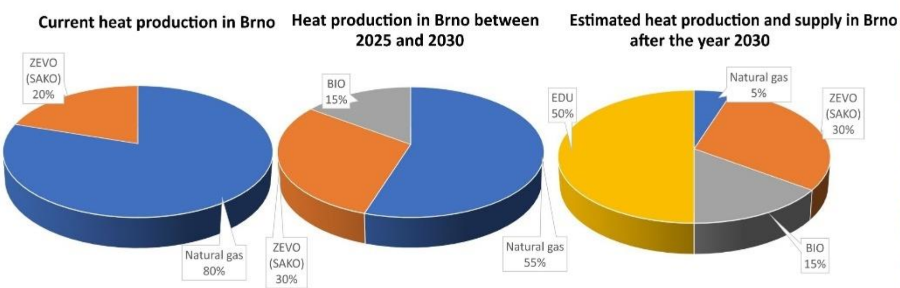

Contact: tomasbab@students.zcu.cz

INTRODUCING SMRs IN THE POWER PRODUCTION OF GREECE

Nikolaidis Nikolaos

School of Electrical and Computer Engineering, Faculty of Engineering, Aristotle University of Thessaloniki, Greece

Greece, as an EU member state, attempts to achieve the goal of Fit-for-55 program by decreasing the energy generated from fossil fuel power stations (FFPPs). The objective of this study is to examine the energetic competitiveness of five appropriately selected SMRs compared to Greece's operational coal. The analysis of daily and monthly distribution of generated energy of the previous year was conducted to demonstrate the potential insertion of SMRs in Greece's electrical grid. The outcome will answer the question whether the deployment of a SMR is energetically beneficial for our country.

Introducing SMRs in the Power Production of Greece

Author: Nikolaidis Nikolaos[1] **Supervisor Professor:** Ioannis Kaissas [1]

[1.] School of Electrical and Computer Engineering, Faculty of Engineering, Aristotle University of Thessaloniki, 54124 Thessaloniki, Greece

ARISTOTLE UNIVERSITY OF THESSALONIKI

Introduction

The growing development of Small Modular Reactors (SMRs) and the need for clean energy, substituting power sources that emit CO_2. The developed countries rethink the use of Nuclear Energy as a carbon-free source that could produce a considerable amount of energy. The European Council adopts the Fit-for-55 program, which aims to reduce greenhouse gas emissions by 55% by the year 2030 and achieve total carbon neutrality by 2050[1]. Greece, as an EU member state, attempts to achieve that goal by decreasing the energy generated from fossil fuel power stations (FFPPs). The objective of this study is to examine the energetic competitiveness of five appropriately selected SMRs compared to Greece's operational coal. The analysis of daily and monthly distribution of generated energy of the previous year was conducted to demonstrate the potential insertion of SMRs in Greece's electrical grid. The outcome will answer the question whether the deployment of a SMR is energetically beneficial for our country.

Power Generation in Greece

According to IPTO/ADMIE [2], the annual demand is approximately 50 TWh. From this, Fossil Fuels Power Plants produce 20 TWh annually.

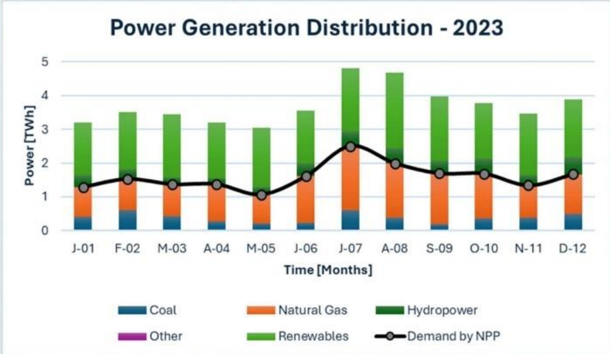

Figure 1. Monthly distribution of the total Power Generation during the year 2023. The curve indicates the power that SMRs could replace.

Operating Modes of an SMR

There are four operating modes [3] of an SMR:

- Base-Load Mode
- Primary frequency control mode: ±2% of nominal power
- Secondary frequency control mode: ±5% of nominal power
- Load-Following Mode: Typically, 50-100% of nominal power

Suitable SMRs

Although, there are plenty of factors that contribute to the selection of the final SMR, one significant factor is the ability to operate in load-following mode.

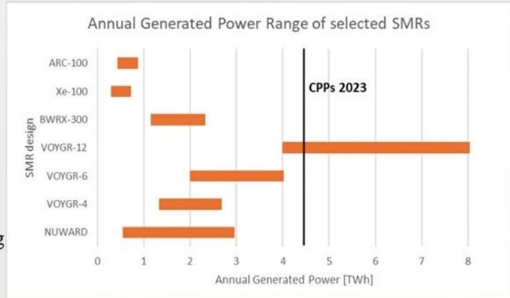

Figure 2. Range of annual possible Generated Power by the SMRs under consideration[4]. The line represents the total annual production from CPPs (Coal) during 2023.

Power Generation with a selected SMR

The day with the **greatest** electricity demand in 2023, was **Friday, 21 July 2023** [2]. The total generated power was 143 MWe.

The assumption for the calculation is that a possible SMR would operate at 95% of its nominal power from midnight to 3 am, then 80% of its nominal power from 3 am to 1 pm and again at 95% from 1 pm to midnight. This is applied to all selected SMRs except Xe-100 and ARC-100 for which we assumed that operate in base-load mode at 95% of their nominal power.

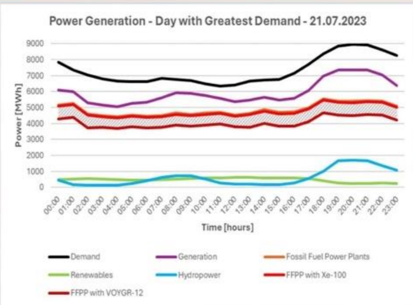

Detail

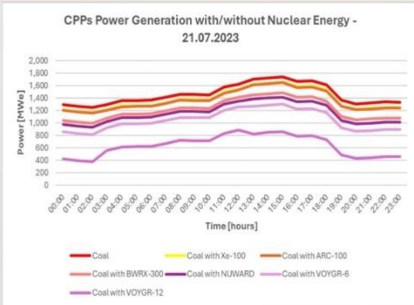

Figure 3. The outlined part is the potential area of power generated by FFPPs if one of the selected SMRs was installed in the electric grid.
Figure 4. Detail of Figure 3 – The total reduction of the curve is proportional to the power production of the selected SMR.

The day with the **lowest** electricity demand in 2023, was **Sunday, 26 March 2023** [2]. The total demand was reduced rapidly from 7 am to 3 pm.

The assumption for the calculation is that a possible SMR would operate at 60% of its nominal power from midnight to 7 am, then 60% until 4 pm and again at 60% from 4 pm to midnight. This is applied to all selected SMRs except Xe-100 and ARC-100 which we assumed that operate in base-load mode at 60% of their nominal power.

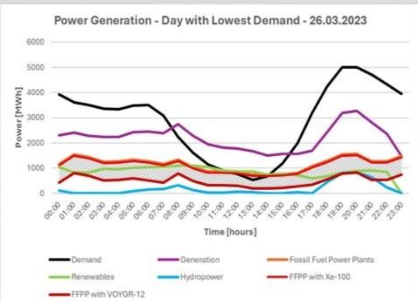

Detail

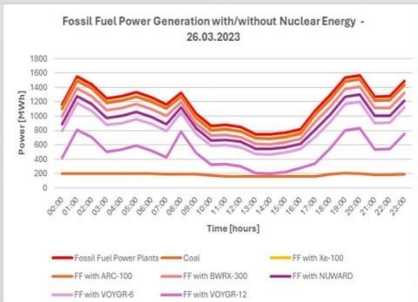

Figure 5. The outlined part is the potential area of power generated by FFPPs if one of the selected SMRs was installed in the electric grid.
Figure 6. Detail of Figure 5 – The energy produced by any SMR will surpass the total generated power of all CPPs.

Conclusions

Calculations on IPT's data [2] showed that the total demand of the country's grid is significant, while the domestic generation of power is reliant on FFPPs. The operation of an SMR, in either load-following or base-load mode, would reduce the total production of power from FFPPs (55.6% to 36.6%), and eventually decrease the total amount of gas emissions. As a result, the deployment of SMRs in Greece is energetically beneficial. Long-term environmental, economical and social aspects have to be considered.

References

[1]. European Council – Counsil of European Union (2024) Fit for 55. https://www.consilium.europa.eu/en/policies/green-deal/fit-for-55/#:~:text=Fit%20for%2055%20refers%20to,line%20with%20the%202030%20goal.
[2] Data extracted from IPTO/ADMIE. https://www.admie.gr/agora/enimerotika-deltia/miniaia-deltia-energeias
[3] Technical and Economic Aspects of Load Following with Nuclear Power Plants, NEA, June 2011
[4] Advances in Small Modular Reactor Technology Developments – A Supplement to: IAEA Advanced Reactors Information System (ARIS) – 2022 Edition

Acknowledgment

Data for Power Generation in Greece was collected by Konstantinos Skoumpris.

MULTI-LAYER COATED CLADDING BEHAVIOUR DURING LOSS OF COOLANT ACCIDENT

Michaela Svatošová

Faculty of Nuclear Sciences and Physical Engineering, Czech Technical University in Prague, Czech Republic

To study the high temperature creep behavior of coated zirconium alloys, a series of ballooning and burst tests was performed. The main focus was on comparing the time to burst and deformation of samples with various types of coating and reference uncoated samples.

Multi-layer Coated Cladding Behaviour during Loss of Coolant Accident

M. Svatošová[1,2], J. Krejčí[1], M. Ševeček[2]

[1] UJP PRAHA a.s., Nad Kamínkou 1345, 156 10 Praha - Zbraslav, Czech Republic
[2] Faculty of Nuclear Sciences and Physical Engineering, Czech Technical University in Prague, V Holešovičkách 2, 180 00 Praha 8, Czech Republic

1. Introduction

During Loss-of-coolant accident the nuclear fuel is exposed to **high temperatures** and **high internal pressure**. This leads to **thermal creep**, i.e. time-dependent plastic deformation. Fuel cladding experiences **ballooning** which may lead to **burst** (failure). [1]

In recent years a lot of research has been focused on various concepts of **Accident Tolerant Fuel (ATF)**, which should have reduced oxidation rade and reduced creep rate (longer time to burst and smaller deformation) during accident conditions. So far, one of the most promising concepts is the deposition of **protective chromium layer** on conventional Zr alloy cladding outer surface. [2-4]

To prevent the interdiffusion of Cr and Zr and their eutetic reaction, it is possible to add an **interlayer of CrN**, as it leads to the creation of ZrN (as depicted in Fig.1), which acts as a diffusion barrier [5].

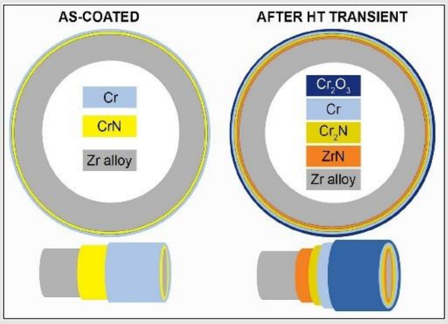

Fig. 1: Multi-layered coating [5]

2. Experimental

2.1 Material

- ❑ Reference uncoated Zr alloy samples
- ❑ Cr coated samples (coating thickness 18.6 μm)
- ❑ Cr coated samples (17 μm)
- ❑ substoichiometric Cr90N10 coated samples (18.2 μm)
- ❑ CrN+Cr coated samples (22.6 μm)
- ❑ CrN+Cr coated samples (16.7 μm)
- ❑ CrN+Cr coated samples with Cr interlayers in CrN (17.6 μm)

2.2 Internal pressure high temperature creep tests

- ❑ Isothermal tests at 750 °C and 950 °C
  - sample heated to high temperature and then pressurized
  - internal pressures 2–10 MPa for 750 °C, 0.9–1.5 MPa for 950 °C
- ❑ Thermal ramp tests at 6 °C/s
  - pressurized sample heated to 360 °C, then temperature increased by 6 °C/s up to the failure of the sample
  - internal pressures 2–10 MPa
- ❑ After the tests the samples were measured in diameter in different places to evaluate their deformation

Fig. 2: Sample before burst test

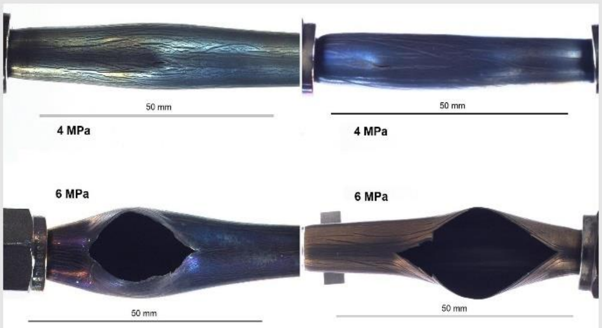

Fig. 3: Samples after burst tests: left – Cr90N10 coated, right – CrN+Cr coated

Acknowledgements: *Financial support of this research through the grant no. TK04030168 of the Technology agency of the Czech republic is gratefully acknowledged.*

3. Results and discussion

3.1 Isothermal tests at 750 °C

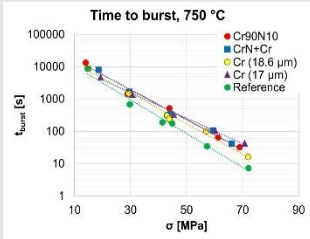

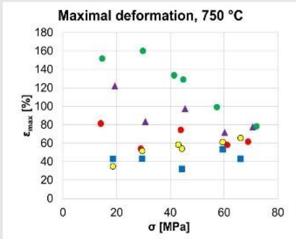

The charts show time to burst and maximal deformation of the sample in relation to hoop stress in the cladding wall. It is clear that coated samples have **longer times to burst** as well as **smaller maximal deformations** than reference uncoated samples. The longest times to burst were in Cr90N10 and CrN+Cr coated samples. The smallest deformations were in Cr (18.6 μm) and CrN+Cr coated samples. These results show the **benefit of coating** in accident conditions, since it leads to less fission gas being released into the reactor pressure vessel area and less flow blockage for water from emergency cooling systems.

3.2 Isothermal tests at 950 °C

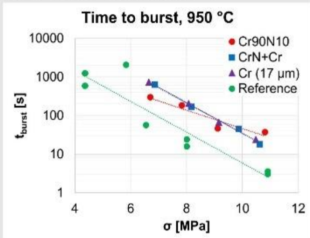

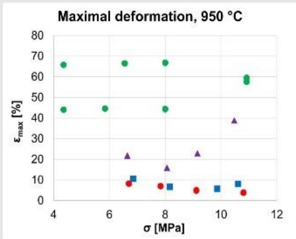

At 950 °C coated samples tended to **fail later** and had **smaller maximal deformations** than reference uncoated samples, which is consistent with results at 750 °C. The benefit of coating has been proved at 950 °C as well.

3.3 Thermal ramp tests

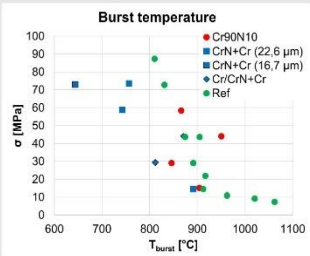

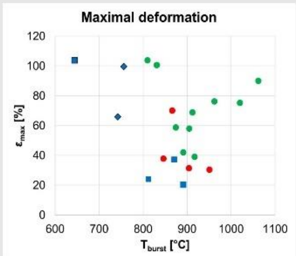

The charts show the relationship of burst temperature and stress in the cladding wall and the maximal deformation. It can be observed that coated samples failed at lower temperatures, which suggests that coated samples **failed earlier**. This is the opposite of what was observed in isothermal tests. This can be explained by the formation of **cracks in the coating** (seen in Fig. 3), which leads to the thinning of the sample wall and concentration of stress in areas around the cracks. However, the maximal deformations are still smaller in coated samples. The benefit of coating in thermal ramp tests is not very straightforward.

4. Conclusions

In isothermal tests the coated samples failed later than reference uncoated samples and had smaller maximal deformations, which means that coated samples have a lower creep rate. Coating has a positive effect on the results of isothermal tests. On the other hand, in thermal ramp tests coated samples failed earlier than reference samples, possibly due to the presence of cracks in the coating, thinning of the cladding wall and concentration of stress in those areas.

References

[1] K. Pettersson et al., "Nuclear Fuel Behaviour in Loss-of-coolant Accident (LOCA) Conditions," OECD Nuclear Energy Agency (NEA), Paris, 2009. NEA No.6846, ISBN 978-92-64-99091-3
[2] "State-of-the-Art Report on Light Water Reactor Accident-Tolerant Fuels," Nuclear Energy Agency, Oct. 2018. doi: 10.1787/9789264308343-en.
[3] K. A. Terrani, "Accident tolerant fuel cladding development: Promise, status, and challenges," Journal of Nuclear Materials, vol. 501, pp. 13–30, Apr. 2018, doi: 10.1016/j.jnucmat.2017.12.043.
[4] J. Krejčí, M. Ševeček, and L. Cvrček, "Development of chromium and chromium nitride coated cladding for VVER reactors," in 2017 Water Reactor Fuel Performance Meeting, Jeju, South Korea, Sep. 2017.
[5] J. Krejčí et al., Development and testing of multicomponent fuel cladding with enhanced accidental performance. Nuclear Engineering and Technology, vol. 52, issue 3, pp. 597–609. ISSN 1738-5733. doi: 10.1016/j.net.2019.08.015.

A CONVOLUTIONAL NEURAL NETWORK APPROACH FOR STEEL SURFACE DEFECT DETECTION IN NUCLEAR FACILITIES

KRISTY GOURAB SINHA

Department of Nuclear Science and Engineering, Military Institute of Science and Technology (MIST), Dhaka, Bangladesh

This research highlights the effectiveness of sophisticated preprocessing techniques and deep learning architectures in the detection of metal surface defects. The detection of surface defects is paramount in both the steel manufacturing and nuclear industries, as it directly affects product quality, production efficiency, and operational safety. The study underscores the importance of model architecture and preprocessing methods in achieving high classification accuracy.

A CONVOLUTIONAL NEURAL NETWORK APPROACH FOR STEEL SURFACE DEFECT DETECTION IN NUCLEAR FACILITIES

AUTHORS

KRISTY GOURAB SINHA
FAIYAZ NOOR

AFFILIATIONS

DEPARTMENT OF NUCLEAR SCIENCE AND ENGINEERING, MILITARY INSTITUTE OF SCIENCE AND TECHNOLOGY (MIST), DHAKA, BANGLADESH.
DEPARTMENT OF BIOMEDICAL ENGINEERING, MILITARY INSTITUTE OF SCIENCE AND TECHNOLOGY (MIST), DHAKA, BANGLADESH.

INTRODUCTION

The detection of surface defects is paramount in both the steel manufacturing and nuclear industries, as it directly affects product quality, production efficiency, and operational safety. Traditional quality control methods are hampered by the lack of real-time diagnostic capabilities, being less automated and unreliable in defect detection. Manual inspections, particularly in nuclear facilities, are challenging due to high heat and radiation concerns, necessitating remote reviews and manual detection which are time-consuming and difficult. This study introduces an advanced approach for defect detection utilizing a deep structured neural network, specifically a Convolutional Neural Network (CNN) combined with class activation maps. Our method enhances the CNN model to analyze and localize defect regions within images, supporting real-time visual decision-making. The CNN classification model is designed to capture high-dimensional spatial features, distinguishing among six different types of surface defects: rolled-in scale, patches, crazing, pitted surface, inclusion, and scratches. Experimental results show that our proposed method achieves outstanding detection performance, with a test accuracy of 98.61% and an F-1 score near one. This approach promises significant improvements in production efficiency, cost reduction, operational safety, and risk management in both steel production and nuclear facilities.

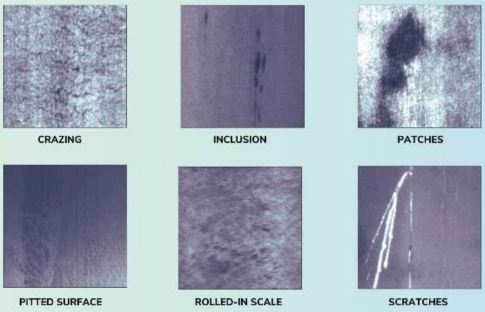

FIG 1: SAMPLE IMAGES FROM ALL 6 CLASSES.

OBJECTIVES

To create an effective preprocessing technique for optimizing image quality prior to analysis. Propose a CNN classification model to classify steel surface defects. Comparing the classification performance with the existing pre-trained model and custom model.

DATASET DESCRIPTION

Class	Training	Validation	Testing	Total
Crazing	276	12	12	300
Patches	276	12	12	300
Scratches	276	12	12	300
Pitted surface	276	12	12	300
Inclusion	276	12	12	300
Rolled-in scale	276	12	12	300
Total	1656	72	72	1800

TABLE 1: CONTENT OF THE DATASET.

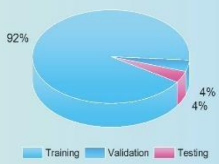

FIGURE 2: DATASET SPLIT.

METHODOLOGY

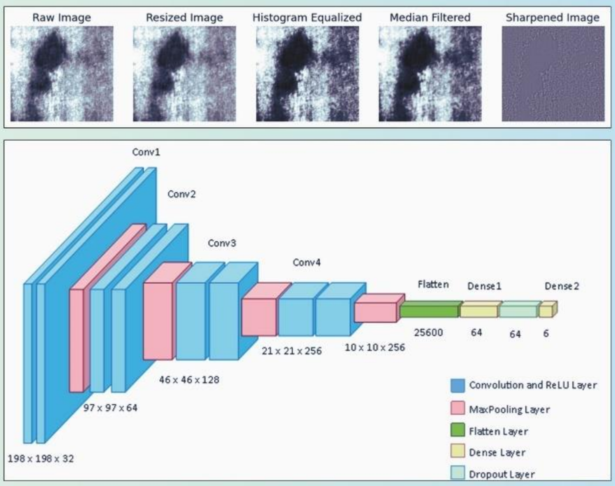

FIG 3: PREPROCESSING PIPELINE AND CNN ARCHITECTURE.

RESULT & PERFORMANCE

Model	Preprocessing method	Epoch	Accuracy (%)	F1-Score	AUC
3 Layers CNN	Raw Data	15	17	0.156	0.49
	GLCM	10	50	0.44	0.77
	Histogram Equalization	10	83.33	0.825	0.97
		50	84.7	0.88	0.98
	Histogram Equalization, Median Filtering, Laplace Sharpening	10	84.7	0.83	0.96
		100	90	0.873	0.98
	Histogram Equalization, Median Filtering, Laplace Sharpening, Adaptive Thresholding	10	76.38	0.7	0.92
4 Layers CNN (Proposed)	Histogram Equalization, Median Filtering, Laplace Sharpening	50	98.61	1.00	1

TABLE 2: PERFORMANCE COMPARISON BETWEEN DIFFERENT PREPROCESSING METHODS AND MODELS.

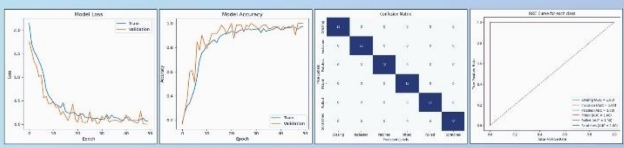

FIG 4: MODEL LOSS, MODEL ACCURACY, CONFUSION MATRIX, ROC CURVE FOR 4 LAYER MODEL WITH HISTOGRAM EQUALIZATION, MEDIAN FILTERING, LAPLACE SHARPENING (50 EPOCHS).

In this study, we explore the performance of Convolutional Neural Networks (CNN) in image classification tasks using various preprocessing methods. We compare models with 3 layers and 4 layers CNN architectures. Initially, raw data yielded suboptimal results, but significant improvements were observed with advanced preprocessing techniques. The combination of Histogram Equalization, Median Filtering, and Laplace Sharpening notably enhanced performance, achieving an accuracy of 90% with a 3-layer CNN. Our proposed 4-layer CNN, further refined with these preprocessing methods, demonstrated exceptional results, achieving 98.61% accuracy, an F1-score of 1.00, and an AUC of 1, showcasing the effectiveness of the proposed architecture and preprocessing techniques.

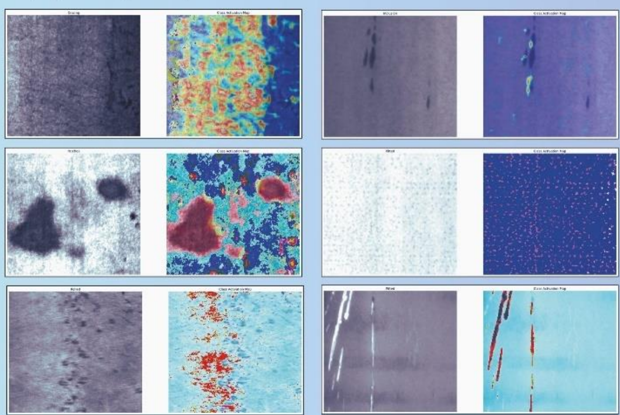

FIG 5: PREPROCESSED IMAGES AND THEIR CLASS ACTIVATION MAPS.

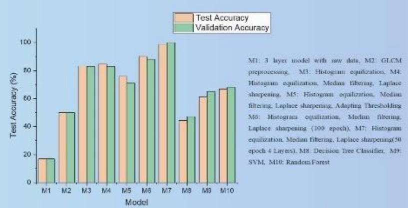

FIG 6: COMPARISON BETWEEN DIFFERENT PREPROCESSING METHODS AND PRETRAINED MODELS

DISCUSSION & CONCLUSIONS

This research highlights the effectiveness of sophisticated preprocessing techniques and deep learning architectures in the detection of metal surface defects. The combination of histogram equalization, median filtering, and Laplace sharpening, along with extended training epochs, significantly boosted model performance. The study underscores the importance of model architecture and preprocessing methods in achieving high classification accuracy. Future research can build on these findings by exploring novel preprocessing methods and further optimizing neural network architectures to push the boundaries of performance and robustness in defect detection models. The comparison with traditional machine learning models further underscores the superiority of deep learning approaches in handling complex classification tasks in this domain.

REFERENCES

Dataset: Song, K.; Yan, Y. A noise robust method based on completed local binary patterns for hot-rolled steel strip surface defects. Appl. Surf. Sci. 2013, 285, 858–864.

MASTER STUDENTS

EXPERIMENTAL DETERMINATION OF THE (A+B) PHASE ZR1NB ALLOY DEFORMATION RATE DEPENDENCE ON WALL STRESS

Andrej Prítrský

Faculty of Mechanical Engineering, Czech Technical University in Prague, Czech Republic

By modifying the burst test setup to measure internal pressure drops, the study provides an analysis of the deformation kinematics as a function of cladding wall stress. The results show the deformation rate dependence of the (α+β)-phase Zr1Nb alloy under different conditions and emphasize its importance for the prediction of cladding behavior during core accidents.

Experimental determination of the (α+β) phase Zr1Nb alloy deformation rate dependence on wall stress.

Andrej Prítrský [1,2]
[1] Czech Technical University in Prague, FME, Technická 4, 160 00 Prague, Czech Republic
[2] UJP PRAHA a.s., Nad Kamínkou 1345, 156 00 Zbraslav, Czech Republic

► Introduction

Accurate assessment of fuel cladding deformation during core accidents, like loss of coolant accidents (LOCA) with core damage, is crucial for predicting fission product release or restoring core cooling. Therefore, the determination of physical properties and behavior in accidental situations, as well as the knowledge of cladding limits, are the subject of numerous research studies, including those conducted at UJP PRAHA a.s. labs.

In the event of a LOCA, it is crucial to restore core cooling in the shortest possible time since the mechanical properties of the fuel cladding change rapidly with temperature.

Burst testing has numerous advantages over tensile testing, the most important of which is that burst testing allows not only axial stress application on the specimen rather than both axial and radial stress.

For this study, specimens were tested in temperatures in range from 750 °C to 850 °C because strain rate in α + β indicates shift from low strain rate α phase to more plastic β phase rates. For Zr1Nb the α + β phase ranges from 760 °C to 940 °C therefore with higher temperatures, the strain rate is rapidly increasing with wall stress.

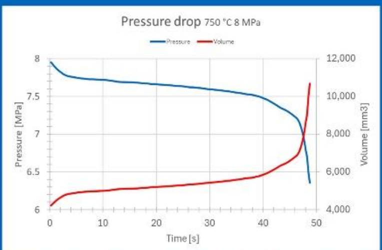

Fig. 1: Internal pressure drop based on shape change.

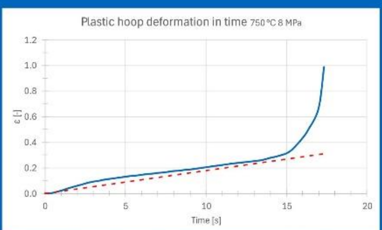

Fig. 2: Comparison of deformation progress in time. Red line is the result of constant gas pressure test blue is constant gas mass test.

► Acknowledgement

This work was supported by the Institutional Support by Ministry of Industry and Trade, Technology Agency of the Czech Republic grant No. TM04000018.

► Methodology

The test is conducted in an electric furnace with controlled temperature and heating rates. The preheated specimen undergo a 15 minute phase stabilization period inside the furnace to ensure exact phase fraction.

The test begins with pressurization of the specimen with inert gas and after full pressurization, the shut off valve (V5) is closed, separating the specimen and gas distribution system. Therefore, a constant gas mass is trapped inside the specimen.

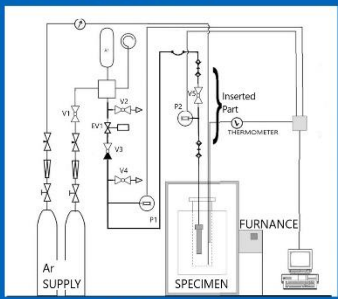

Fig. 3: The testbed

After the specimen deformation occurs, we can calculate the internal volume increase by gas pressure drop.

After the specimen wall rupture occurs, the deformation is measured in various points to describe geometry of the ballooning. We have developed a mathematical model which can describe specimens' deformation over time only from gas pressure drop and terminal deformation.

On figures below we can compare results from constant pressure burst tests (red dashed) and new methodology results (blue).

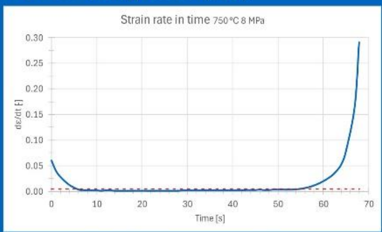

Fig. 4: Strain rate progress in time.

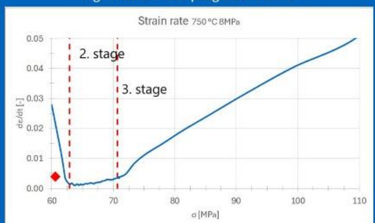

Fig. 5: Strain rate dependence on the in-wall stress

► Results

The results of each experiment consist of a uniform deformation and the maximum deformation of the specimen over time and deformation rate. From this data, we can calculate the 3 directional internal wall stress using only the deformation and internal gas pressure only, and their changes over time.

This is a major improvement over previous burst tests, which could only measure the average deformation over the entire test. Secondary stage creep, in reality, has a lower strain rate than the average strain rate calculated from the constant pressure burst test as shown by the red dashed line. From the constant mass burst test results , we can determine the dependence of the uniform secondary creep strain rate on in-wall stress as shown below with the yellow line.

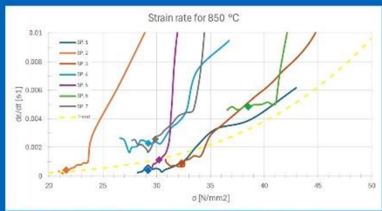

Fig. 6: Strain rate dependency on in-wall stress for 850°C

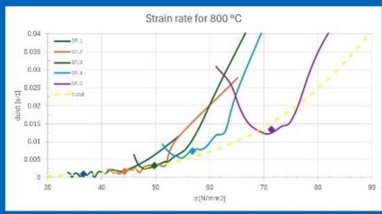

Fig. 7: Strain rate dependency on in-wall stress for 800°C

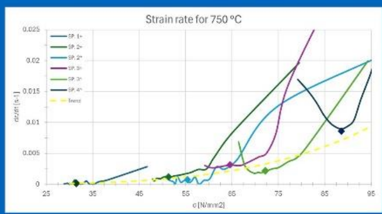

Fig. 8: Strain rate dependency on in-wall stress for 750°C

► Conclusions

The accuracy of the results is not as high as from the tensile test, however, we are able to obtain results at much higher temperatures without the use of expensive machinery. Unlike previously used constant pressure burst tests, which can only provide time-independent data, we are able to observe creep stages, strain rate and in-wall stress growth over time.

[1] D. Kaddour, S. Frechinet, A. F. Gourgues, J. C. Brachet, L. Portier and A. Pineau, "Experimental determination of creep properties of Zirconium alloys together with phase transformation," *Script Materialia*, vol. 51, no. 6, pp. 515-519, 2004.
[2] H. Rosinger, "The Elastic Properties of Zirconium Alloy Feul Cladding and Pressure Tubing Materials," *Journal of Nuclear Materials*, vol. 79, pp. 170-179, 1979.

DESIGN OF THE INTERNAL CIRCUIT OF THE SYSTEM FOR LONG-TERM HEAT REMOVAL FROM NPP HERMETIC ZONE DURING A SEVERE ACCIDENT

Silvie Zemanová

Energy Institute, Faculty of Mechanical Engineering, Brno University of Technology, Czech Republic

Maintaining the highest safety standards requires new ways and means of dealing with emergency situations. The described system for long-term heat removal from the NPP hermetic zone is designed to cope with severe accidents. This system allows start-up without the need for electrical power inside the hermetic zone.

Design of the internal circuit of the system for long-term heat removal from NPP hermetic zone during a severe accident

Ing. Silvie Zemanová

Energy Institute; Faculty of Mechanical Engineering; Brno University of Technology; Czech Republic

https://www.vut.cz/studenti/zav-prace/detail/157183
For further information please visit the link or QR code above.

SEVERE ACCIDENT MANAGEMENT

Severe accidents at nuclear power plants (NPP) are accidents associated with core melting. This in itself entails the loss of the first physical barrier against the escape of fission products – fuel cladding. In the event of a loss of coolant accident, the second physical barrier – the pressure boundary of the primary circuit is also lost, and then the highest priority is to maintain the integrity of the containment. The greatest threats to containment integrity include hydrogen explosion, long-term over-pressurisation and base plate melting. The long-term heat removal system, which design I dealt with in my diploma thesis, is dedicated to protect the containment from over-pressurization and to provide sufficient water level on the floor for core cooling.

DEFENCE IN DEPTH

The fundamental safety strategy in NPP design is the principle of Defence in Depth (DiD), i.e. protection at several independent levels in order to prevent emergency situations. Czech legislation operates in accordance with WENRA with five levels of DiD, as described in the table below.

Second-generation NPP designs (which include the both Czech NPPs) contained safety systems up to level DiD 3a, which ensure the management of the design basis accidents up to the originally maximum design accident – loss of coolant accident with a guillotine cut of the primary circulation pipe.

Therefore, systems for coping with design extended conditions (DEC), and hence severe accidents, are being installed to these power plants years after their commissioning.

LONG-TERM HEAT REMOVAL SYSTEM

Long-term heat removal system is designed to cope with severe accidents and therefore it is part of level DiD 4. The system concerned is designed for WWER 440 and consists of two circuits.

The cooling water of the external circuit (blue in figure below) is used to drive the turbopump and remove heat from the inner circuit.

The inner circuit (red in figure below) located in the hermetic zone draws the hot active medium by the turbopump from the floor through the heat exchanger to the 11th floor of the barbotage tower. Then the medium flows out through the perforated sheet metal, showers the barbotage tower shaft and helps to reduce the pressure by condensing water vapor in the atmosphere. The layout of the pipeline route is designed with respect to the existing technology and minimization of pressure losses. The entire inner circuit operates without the need for an electrical supply and does not require the manipulation of valves inside the hermetic zone, which facilitates the start-up of the system in severe accident conditions.

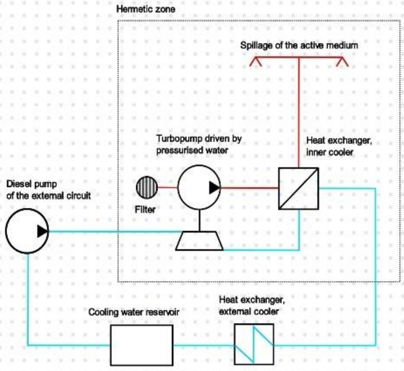

DESIGN OF THE INNER COOLER

Due to the high requirements for durability and reliability of the system, the inner cooler is designed as shell and tube heat exchanger with U-tubes made of austenitic stainless steel 1.4541. The material and wall thickness is designed based on NTD A.S.I., Section II, III. Helical baffle system is used to eliminate fouling. Because of the high heat flow rate required and the limited size, the exchanger is designed to be divided into four modules in a series-parallel arrangement (as in the figure below).

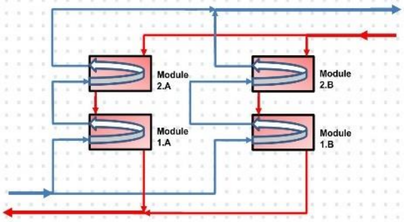

This configuration allows better utilization of the temperature gradient by counter-current arrangement of the modules in series and facilitates transport to the hermetic zone of the operating plant.

The temperature profiles of both media in the heat exchanger in the design state are shown in the graph below.

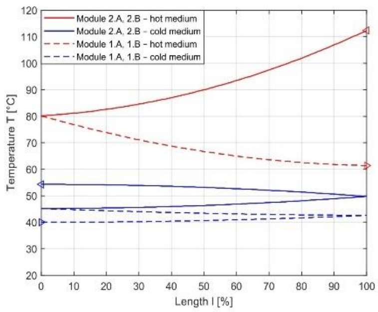

DiD level	Operational state of the unit	Objective
1	Normal operating conditions	Prevention of abnormal conditions
2	Abnormal operating conditions	Prevention of emergency conditions
3a	Design basis accident (DBA)	Prevention of core meltdown
3b	Design extension conditions DEC-A	Prevention of core meltdown
4	Design extension conditions DEC-B	Severe accident management (preservation of existing physical barriers)
5	Essentially eliminated events	Suppression of the consequences of a major radioactive release

OPTIMISATION OF NUCLEAR FUEL FOR USAGE IN SMALL LIGHT WATER CORES

Ondřej Lachout

Czech Technical University, Faculty of Nuclear Sciences and Physical Engineering, Department of Nuclear Reactors, Czech republic

Poster is focused on numerical simulations of nuclear reactors, the preparation of macroscopic nuclear data using a deterministic approach, and the analysis of selected Accident Tolerant Fuel (ATF) concepts of fuel pellets. The concepts analysed in terms of neutronic and safety parameters were compared to the reference UO2 fuel.

OPTIMISATION OF NUCLEAR FUEL FOR USAGE IN SMALL LIGHT WATER CORES

Author: Ondřej Lachout [1]

Co-author: Pavel Suk [1]

[1] Czech Technical University, Faculty of Nuclear Sciences and Physical Engineering, Department of Nuclear Reactors, Czech republic

NUCLEAR DAYS

ABSTRACT

Poster is focused on numerical simulations of nuclear reactors, the preparation of macroscopic nuclear data using a deterministic approach, and the analysis of selected Accident Tolerant Fuel (ATF) concepts of fuel pellets. The behaviour of ATFs in large cores has already been investigated in depth, but analyses in small cores have not yet been studied in more detail. Macroscopic nuclear data were prepared using the SCALE-Triton computational code on an infinite fuel assembly model. Subsequently, a 3D full-core calculation is performed in the deterministic macrocode PARCS on the model of a light-water Small Modular Reactor (SMR) developed by the NuScale Power company. The behaviour of selected ATFs and deviations of various neutronic parameters from the referenced UO_2 fuel are analysed in this complex model. Together with the analyses, a proposal on the optimisation of the referenced core was performed.

DETERMINISTIC DATA PREPARATION

The whole process, from the preparation of templates for lattice code to the execution of the full-core calculation in deterministic macrocode, is a very extensive task and requires an interaction among a group of computational programmes and scripts, allowing proper communication and data transfer between them.

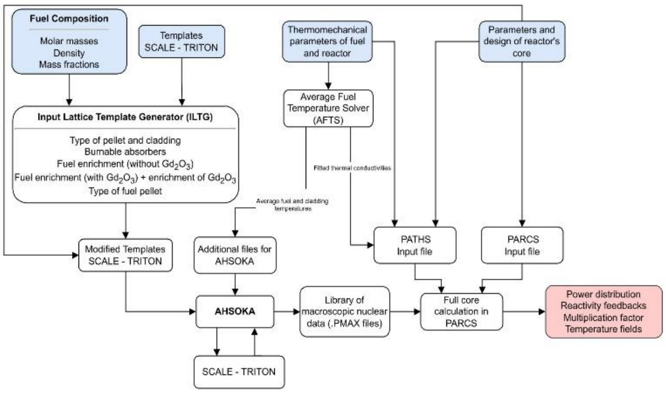

Fig. 1 - Schematic representation of deterministic data preparation and calculation process.

Since we are dealing with different types of fuel pellets, having various thermal conductivities, therefore, different average fuel temperatures, a simple script called Average Fuel Temperature Solver (AFTS) was implemented. This script supports and increases the precision of data preparation for various fuel concepts.

FULL CORE CALCULATIONS

Full-core calculations for nuclear reactors are performed for safety report and optimisation of fuel loading pattern. With respect to the high dependence on calculation time, less demanding deterministic macrocodes are used to provide these calculations. Deterministic macrocode PARCS was chosen for full-core neutronic analysis.

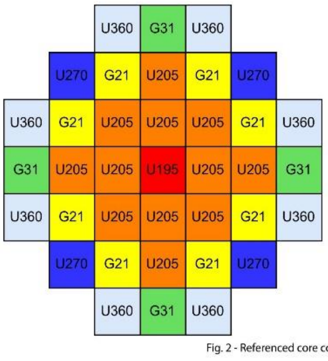

U195 - 1.95% uniformly enriched fuel pins
U205 - 2.05% uniformly enriched fuel pins
U270 - 2.05% uniformly enriched fuel pins
U360 - 2.05% uniformly enriched fuel pins
G21 - 256 fuel pins enriched to 2.7 %, 8 pins enriched to 1.8 % with 2.5 % of Gd absorber
G31 - 256 fuel pins enriched to 3.6 %, 8 pins enriched to 1.5 % with 3.0 % of Gd absorber

Fig. 2 - Referenced core configuration of NuScale reactor.

FUEL PELLETS COMPARISON

The thermomechanical parameters of the fuel pellets analysed are summarised in Table 1. To highlight the advantage of the higher density and actinides fraction of some concepts, the masses of fuel and actinides in a NuScale's fuel assembly are presented in Figure 3.

For proper concepts comparison, the referenced reactor thermal power (P_{ref} = 160 MWt) was fixed. To follow this condition, specific powers (P_{spec}) for different concepts had to be determined using the relation (1).

$$P_{\text{spec}} = \frac{P_{\text{ref}}}{m_{\text{f}}}, \tag{1}$$

where m_f is the total mass of fuel in the reactor.

Tab. 1 - General parameters of analysed fuel pellets.

	Actinides[a] [wt. %]	m_f[b] [kg]	P_{spec} [W g^{-1}]	$\overline{T}_f$ [K]	T_f^{max} [K]
UO2	88.1	249	17.33	699	772
U3Si2	92.7	278	15.57	663	696
UN	94.1	326	13.26	649	668
U10Mo	90.3	390	11.08	643	656
UO2BeO	76.2	225	19.25	642	654
MOX(U)	87.2	252	17.16	708	789
ThO2	87.9	228	18.94	682	736

[a] Mass fraction of actinides in fuel (isotopes U a Pu).

[b] Fuel mass in a fuel assembly.

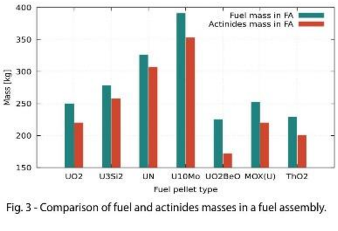

Fig. 3 - Comparison of fuel and actinides masses in a fuel assembly.

NEUTRONIC CALCULATIONS RESULTS

From a neutronic point of view, all previously mentioned fuel concepts were studied in combination with M5 cladding on the NuScale reactor model in the deterministic macrocode PARCS with the external T/H solver PATHS. Individual fuel concepts were compared with reference UO_2 in terms of various neutronic and safety parameters. These parameters include:

- Fuel campaign length,
- safety parameters,
- power distribution.

Fuel Campaign Length

For some fuel concepts, the fuel campaign can be extended due to the higher fuel density and weight fraction of the fissile material. Graphically, the dependence of the critical boron concentration in the moderator on the burnup is shown in Figure 4.

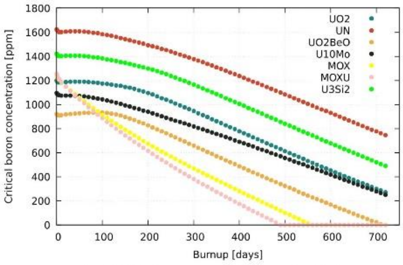

Fig. 4 - Critical boron concentration for analysed fuels.

Safety Parameters

Two neutronic parameters related to safe reactor operation were studied:

- Effective delayed neutron fraction,
- reactivity coefficient by increase of inlet coolant temperature.

The effective delayed neutron fraction is given directly by the PARCS output file. For the reactivity coefficient the temperature of the inlet coolant was increased by ΔT and together with the change in reactivity Δρ was substituted in the formula (2) representing the direction of a linear function.

$$\alpha_{\text{T}^{\text{M}}} = \frac{\Delta\rho}{\Delta T}. \tag{2}$$

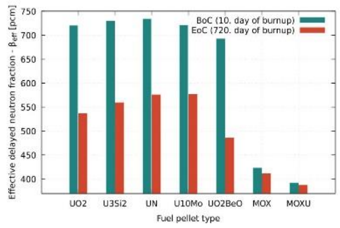

Fig. 5 - Effective delayed neutron fraction.

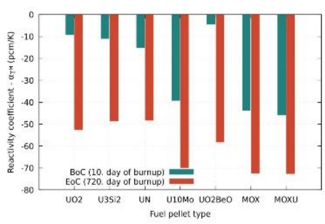

Fig. 6 - Moderator reactivity coefficient.

Power Distribution

For the purposes of this study, the maximal peaking factors (PF_{max}) are defined as the nodes/parts of fuel pin (both axial and radial), which are the most power-loaded (see equation (3)).

$$\text{PF}_{\max} = \frac{P_{\max}}{\overline{P}}, \tag{3}$$

where P_{max} is a most power loaded node/part of fuel pin and P is an average power loaded node.

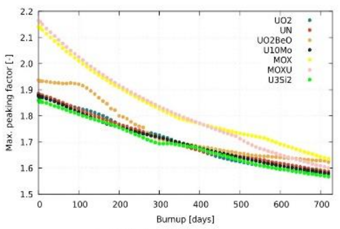

Fig. 7 - Maximum PF over burnup.

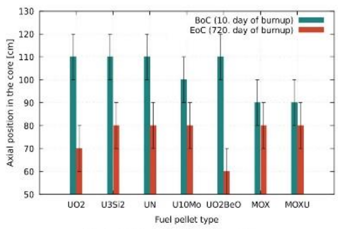

Fig. 8 - Axial position of maximal PF.

CONCLUSION

The concepts analysed in terms of neutronic and safety parameters were compared to the reference UO_2 fuel. For UN and U_3Si_2 fuel pellets, due to the higher fuel density and the higher mass of the fissile material, the fuel campaign can be extended or the average enrichment of the reactor core could be reduced. From the point of view of both the operational and safety parameters, it proved impossible to operate the reactor uniquely with MOX(U) fuel. These fuels are characterised by a significantly lower value of the effective fraction of delayed neutrons and higher maximum value of PF. For all concepts, the axial and radial distribution of PF in the core was investigated. PFs are mainly located near the edges of FAs and near the guide tubes. These locations are power-loaded mainly because of better neutron moderation. As burnup progresses, the values of PF decrease, and the most loaded nodes of FP move to the lower half of the core.

VERIFICATION OF THE QUALIFIED NODALIZATION OF THE TABLE TOP FACILITY

Valentin Roch

Belgian Nuclear Research Centre, SCK CEN, Mol, Belgium

The main goal of the MYRRHA reactor is to transmute minor actinides in order to reduce the radiotoxicity of nuclear wastes in Belgium. This poster deals with the verification of the numerical model of the experiment in SCK CEN (the Belgian Nuclear Research Center) assessing the geometry of MYRRHA's heat exchangers. The results obtained are quite promising for the future of the project.

Verification of the qualified nodalization of the Table Top facility

Author: Valentin Roch | Mentor: Davide Rozzia Belgian Nuclear Research Centre, SCK CEN, Mol, Belgium **E-mail: val.roch@orange.fr**

Introduction

The reactor **MYRRHA** (Multi-Purpose hYbrid Research Reactor for High-tech Applications) is under development at SCK CEN. This fast spectrum reactor will use a **Lead-Bismuth Eutectic (LBE)** as primary coolant and will be the first accelerator driven system. Its goals will be to serve as Gen IV demonstrator and will be able to transmute minor actinides, produce radioisotopes for medicine and cancer treatment and to develop fusion and fundamental research.

The **Table Top** facility has been developed in SCK CEN in order to assess the unique geometry of a **Primary Heat eXchangers (PHX)** tube. It is a steam-water open loop operating under natural circulation that will provide experimental data for thermal hydraulics code assessment and model development on top of evaluating its thermal resistance.

Ref. [3][4]

Objectives

- ❑ O1: Refine existing **RELAP5/mod3.3** nodalization
- ❑ O2: Verify it against different tests
- ❑ O3: Predict Table Top behavior with a leak

Exp.	Leak?
RUN#8.1	✗
RUN#11.1	✗
RUN#7	💧
RUN#8	💧

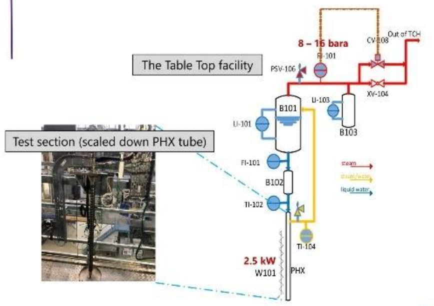

O1: R5 3.3 input deck modification

Exp.	Leak?
RUN#8.1	✗
RUN#11.1	✗

- New **boundary conditions** (BC) were imposed at **vessel B103** due to unphysical values met by the fluid temperature inside it. This is due to the impossibility for RELAP to model axial conduction.

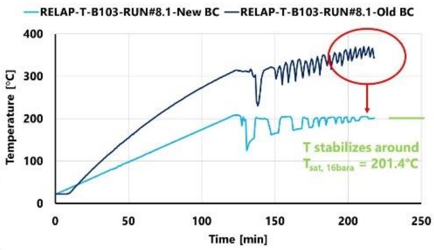

Old BC	Power of electrical heat tracing + imposed heat transfer coefficient (HTC)
New BC	Average vessel surface temp. + infinite HTC

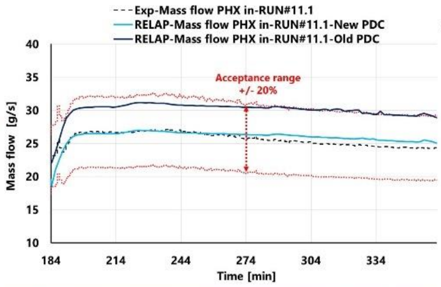

- A more accurate **pressure drop coefficient (PDC)** was also applied for each ring inside the **riser tube**. In this way, the computed PHX inlet mass flow rate better fits the experimental one during the steady-state.

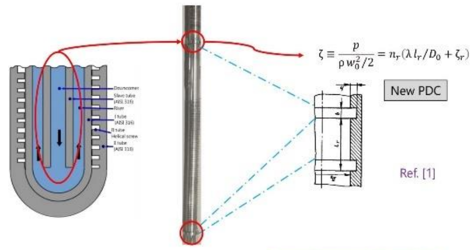

Ref. [1]

O2: Verification of the acceptance criteria

Exp.	Leak?
RUN#8.1	✗
RUN#11.1	✗

The **8** acceptance criteria defined for the **transient** (1-16 bara), the **steady-state** (16 bara) and the **heat losses (HL)** are met for RUN#8.1 and 11.1, e.g.:

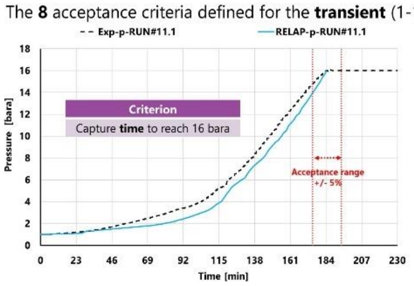

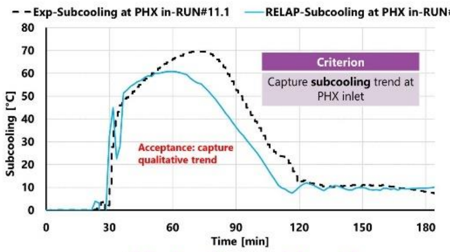

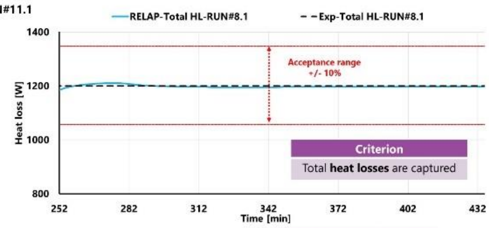

O3: Leak consideration

Exp.	Leak?
RUN#7	💧
RUN#8	💧

The leak detected at the valve **CV 108** during RUN#7 and 8 was modeled with the addition of a "leak line" in the nodalization. The diameter of pipe 181 (~ **90 µm**) was computed to fit the experimental leak mass flow rate. In this way RUN#7 and 8 meet all of the acceptance criteria.

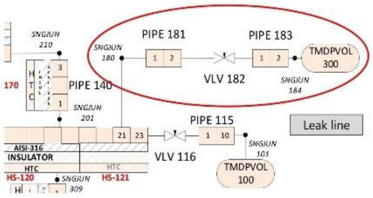

Measured leak N_2 6.1 bara (mbar.l/s)	Measured leak sat. steam 16 bara (mbar.l/s)	Measured leak sat. steam 16 bara (kg/s)
3.32	26.18	1.19E-05

$$\frac{Q_A}{Q_B} = \left(\frac{\eta_B}{\eta_A}\right)\left(\frac{P_1^2 - P_2^2}{P_3^2 - P_4^2}\right)$$

$$Q_{turb} = \pi d^{5/2}\left[\frac{g R_0 T (P_1^2 - P_2^2)}{64 f M l}\right]^{1/2}$$

$$N_{Re} = \frac{Q}{d}\frac{4M}{\pi \eta R_0 T} = \frac{\rho d F}{\eta}$$

Ref. [2]

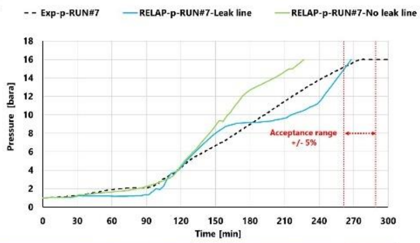

Conclusion

- ☑ O1: More physical & accurate model
- ☑ O2: Matching of all 8 criteria
- ☑ O3: Matching criteria with leak line

Perspectives

- Assessment of the **draining phase** of Table Top (boiling at atmospheric pressure, to avoid corrosion in-between experiments): tricky due to the occurrence of complex physical phenomena such as dry-out and instabilities. Gives adequate results so far but should be investigated by a dedicated study.
- Operation of **HEXACOM** (testing a full-scale PHX tube heated by a LBE loop)

[1]: Idelchick, I.E. (2007). Handbook of hydraulic resistance. 4th revised and augmented version. William Begell: New York.
[2]: Peters, P.H. (1969). Leakage testing handbook. Revised edition. General Electric R&D: New York.
[3]: Hamid Aït Abderrahim, Peter Baeten, Didier De Bruyn, Rafael Fernandez (2012) MYRRHA – A multi-purpose fast spectrum research reactor. *Energy Conversion and Management*, Volume 63, Pages 4-10. ISSN: 0196-8904. Available at: https://doi.org/10.1016/j.enconman.2012.02.025.
[4]: Dikominos Makris, L. (2024). Analysis of Table Top experiments by means of thermal-hydraulic system code. MSc thesis in nuclear engineering. Politecnico Milano.
[5]: Information Systems Laboratories, Inc. Nuclear Safety Analysis Division (June 2004). RELAP5/mod3.3 code manual. Volume II: Appendix A - Input requirements.

TEPLATOR SMR'S ELECTRICAL EQUIPMENT DESIGN

Jan Ullmann

Faculty of Electrical Engineering, University of West Bohemia, Czech Republic

The poster is dealing with electrical parts of the SMR TEPLATOR. Thesis define legislative and normative requirements for designing electrical power supply. The final part of the poster/thesis deals with a final design of the electrical power supply concept.

TEPLATOR SMR´S ELECTRICAL EQUIPMENT DESIGN

FACULTY OF ELECTRICAL ENGINEERING
UNIVERSITY OF WEST BOHEMIA

Author: Ing. Jan Ullmann

Diploma thesis supervisor: Ing. Jana Jiřičková, Ph.D.

Consultant: Ing. David Mašata

JADERNÉ DNY

INTRODUCTION

The thesis deals with the **DESIGN OF THE ELECTRICAL PARTS** of the **SMR TEPLATOR**. In the current stage of development, only the nuclear parts around the nuclear reactor have been developed. This thesis deals with the **design of the electrical concept of the power supply** of the individual systems. Part of the thesis is a description of the individual parts of the **SMR TEPLATOR**, which are important in terms of electrical power supply. Subsequently, the thesis defines the **LEGISLATIVE AND NORMATIVE REQUIREMENTS** for constructing nuclear facilities regarding **electrical power supply**. Then, the individual facilities considered are categorized according to the importance of the electrical supply. The final part of the thesis deals with the **DESIGN OF THE ELECTRICAL CONCEPT**.

Fig.1 TEPLATOR TECHNOLOGY

DIVISIONS DESIGN

In terms of electrical power supply design, it is very important to divide the individual devices into **power supply categories:**

- **CATEGORY I**

Require uninterrupted power supply, battery-powered in case of power failure.

- **CATEGORY II**

Allow power outages for a few seconds, after starting the backup diesel generators the power is restored.

- **CATEGORY III**

Power is not restored to these devices.

PRACTICAL DESIGN

During the design of the electrical part, the sizes of the **individual transformers and then the cross sections of the individual cables were dimensioned**. The system was calculated in a script created in **Matlab and then validated using DNCalc** (this program is usually used for checking short-circuit ratios). The work also included **dimensioning the size of the diesegenerators** and a procedure for designing the batteries. **Fig.2 shows a simplified diagram of the electrical supply of the TEPLATOR system.**

CONTROL OF POWER SYSTEM

After the design of the electrical system, several control calculations were made:

- Check for short circuit resistance
- Load control of individual transformers
- Check for voltage drop on the transformer (Start-up check of the largest drive and the group of self-starter motors)

Contact: ullmann@students.zcu.cz

TEPLATOR ELECTRICAL EQUIPMENT

In the current state of development, the largest pumps and instrumentation and control systems, together with the power supply for the valves, are considered for the sizing of the electrical power supply.

- **Reactor coolant pump**
- **Emergency core cooling injection pumps**
- **Containment spray pump**
- **Moderator circulating pump**
- **Secondary pumps**
- **I&C, Power supply for valves and drives**

LEGISLATIVE AND NORMATIVE REQUIREMENTS

In the thesis, three sources are considered as a theoretical basis for the subsequent design of the electrical part.

- Requirements for nuclear facility design (based on Decree No. 329/2017 Coll, SÚJB)
- Electrical power supply design of an industrial plant (ČSN 341610)
- Own consumption of thermal power plants and heating Plants (ČSN 38 1120)
- Calculation of short-circuit currents (for cable sizing control - ČSN EN 60909-0 ed.2)

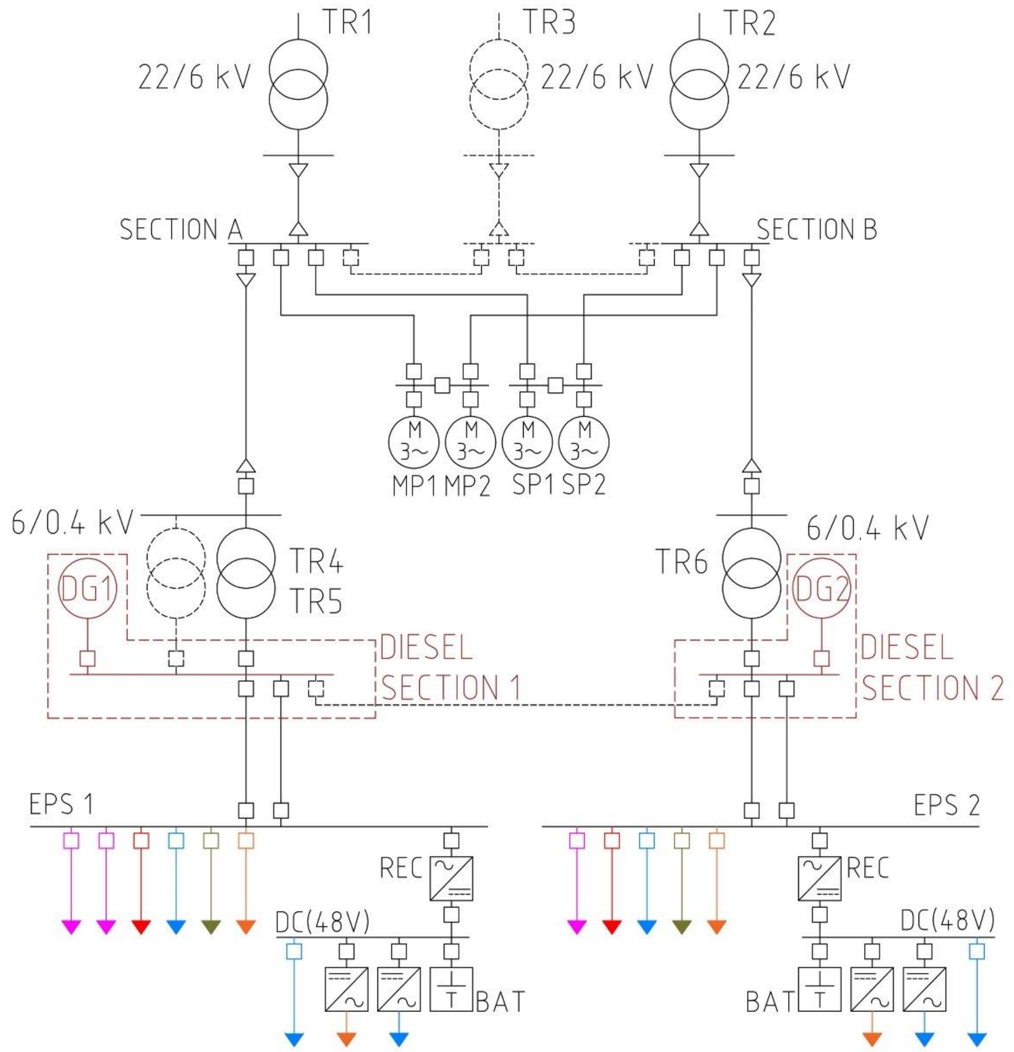

Fig.2 SIMPLIFIED DIAGRAM OF THE TEPLATOR ELECTRICAL EQUIPMENT DESIGN

CONCLUSION

The thesis provides an overview of the **SMR TEPLATOR** system in terms of the electrical supply of individual devices. It presents a comprehensive view of the **legislative and normative requirements** for these systems. The thesis also includes the **design of the individual power supply categories** and the assignment of individual devices. The final part of the thesis is the **design of the electrical supply, dimensioning of individual transformers, cable cross sections** etc. has been carried out. Subsequently, the **controls of the power supplies** were done. **The thesis and the design itself can serve as a basis for the creation of the power supply of the TEPLATOR system in the future.**

THERMAL-HYDRAULIC TRANSIENT ANALYSIS OF DEDICATED DEPRESSURIZATION SYSTEM FOR GEN-III+ PWR IN STATION BLACKOUT

Sana Jamal

Department of Nuclear Engineering, Pakistan Institute of Engineering and Applied Sciences (PIEAS), Pakistan

To analyze the effectiveness of the Dedicated Depressurization System (DDS) in Gen-III nuclear reactors during a station blackout (SBO), a transient model for the ACP1000 design was developed using the MELCOR code. The study focused on simulating the severe accident scenarios, evaluating the DDS's effectiveness in mitigating risks of high pressure melt ejection and direct containment heating.

Thermal-Hydraulic Transient Analysis of Dedicated Depressurization System for Gen-III+ PWR in Station Blackout

Candidate: ***Sana Jamal*** [a]   *Project Duration: 2023-24*

Supervisor: ***Abu Bakar***, *Co-supervisors:* ***Dr. Muhammad Ilyas*** , ***Salik Javaid***

[a] Department of Nuclear Engineering, Pakistan Institute of Engineering and Applied Sciences (PIEAS), Pakistan

Introduction & Motivation

- Station Blackout (SBO) is a severe accident in NPPs: leads to direct containment heating (DCH) by high pressure melt ejection (HPME) of molten corium from RPV.
- The Dedicated Depressurization System (DDS) mitigates these risks by depressurizing the RPV, reducing molten material and minimizing DCH effects.
- Motivated by the Fukushima accident, DDS is crucial in Gen-III+ NPPs to ensure reactor safety during core meltdowns.

Project Objectives

1. **Development of a transient model** for 1100 MWe ACP1000 design using MELCOR code.
2. **Severe accident process analysis** by simulation of station blackout and resulting control parameters.
3. **Validate effectiveness of DDS** through thermal hydraulic analysis of RPV and containment.
4. **Validation of MELCOR model** for future applications to other accident scenarios.

Severe Accident Transients

SBO { DEC-B accident }

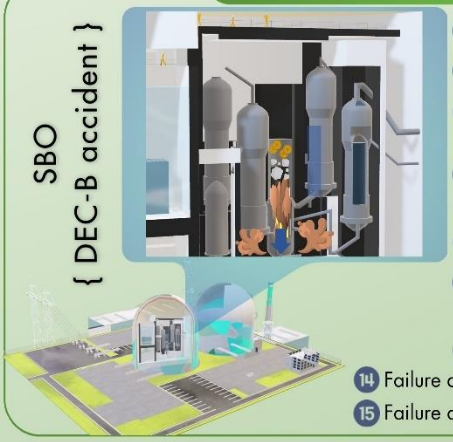

1. Loss of all AC power
2. Reactor trip
3. SG safety valves open
4. SG depletion
5. Core uncovery
6. Core outlet temperature > 650°C
7. Accumulators injection
8. Cladding oxidation and fuel failure
9. Loss of core geometry
10. RPV dry-out
11. Corium relocation to lower head
12. RPV failure
13. RPV failure consequences:
14. Failure at low RPV pressure — No HPME occurs
15. Failure at high RPV pressure — HPME (DCH) occurs

DDS for ACP1000 Reactor

- Level 4 defense-in-depth.
- Set of motorized valves connected to pressurizer.
- Powered by DC batteries.
- Fast-depressurization of RCS.
- Actuated manually by operator, when core exit temperature > 650°C for more than 60 mins.
- Prevents HPME by reducing RCS pressure to less than 2 MPa and protects containment integrity.

Methodology & Nodalization

Modelling Process:

MELCOR Input Packages Used For Analysis:

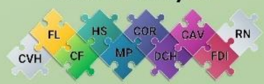

Input Parameters:

Reactor thermal power	3,050 MWth
Pressurizer pressure	15.5 MPa
Reactor coolant flow rate	68,520 m3/h
Number of fuel rods	177 x 264
Core inlet temperature	291.5 C
Core outlet temperature	381.8 C
Main steam flow rate	1,700 kg/s

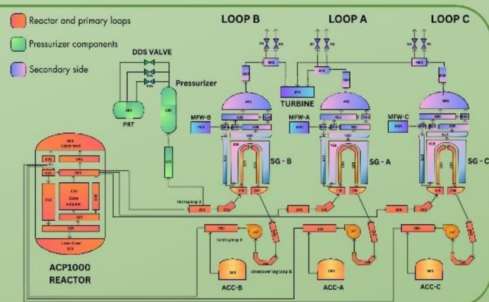

Results & Transient Analysis

— **Case 1:** DDS valves opened by operator

— **Case 2:** DDS valves not opened

{ RPV Water Level }

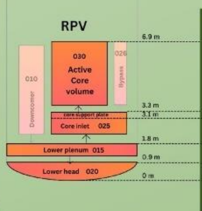

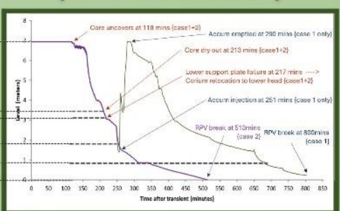

{ Core Exit Temperature }

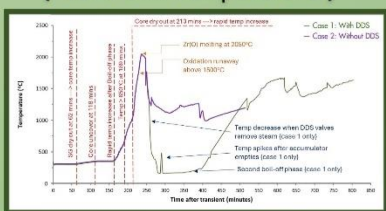

{ RCS Pressure }

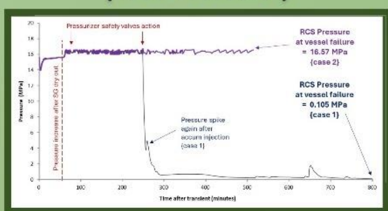

Conclusions

- Station blackout without any heat removal and , leads to core meltdown and reactor vessel failure.
- Without reactor depressurization, a high pressure melt ejection (HPME) occurs. Corium releases from RPV with > 16 MPa pressure and thus containment integrity is at risk due to direct containment heating (DCH).
- The Dedicated Depressurization System can prevent HPME by lowering RCS pressure to < 2 MPa before RPV failure.

Events	Case 1: No DDS	Case 2: DDS actuated
Core uncover time	118 mins	118 mins
CET reaches 650 C	189 mins	189 mins
DDS actuation	---	249 mins
RPV failure / Lower head break	513 mins	800 mins
RCS pressure when RPV failure	16.57 MPa	0.105 MPa

References

- *ELearning Module on Severe Accidents, IAEA (2023). Available at: https://www.iaea.org/online-learning/courses/1537/elearning-module-on-severe-accidents*
- *Approaches and tools for severe accident analysis for nuclear power plants. IAEA Safety Reports Series No. 56 (2008).*
- *Accident management programmes for nuclear power plants. IAEA Safety Standards Series No. SSG-54 (2019).*

Learn all about NPP severe accident analysis: linktr.ee/sanajamal

NUCLEAR DAYS 2024

Sana Jamal, MSc nuclear engineering, sanajamal0111@gmail.com

INFLUENCE OF COOLANT TEMPERATURE ON THE QUENCH FRONT VELOCITY

Martin Štyks

Czech Technical University in Prague, Czech Republic

This thesis deals with the quenching phenomenon and its application during LOCA events in nuclear reactors. A set of experiments is conducted to study and observe this phenomenon using a modified experimental setup designed for bottom flooding of a vertical channel.

Influence of coolant temperature on the quench front velocity

Martin Štyks[1]
stykmar@gmail.com
[1]Czech Technical University in Prague, FME, Technická 4, 160 00 Prague, Czech Republic

Introduction

Quenching is a phenomenon in the field of heat transfer which has been known and used for a very long time in materials science. In recent years extensive studies have been carried out in connection with quenching in nuclear reactors due to its impact on nuclear safety. Quenching is defined as rapid cooling of very hot surfaces with a relatively cold liquid. If the surface temperature is high enough, liquid is evaporated immediately after reaching the surface. Stable vapour layer is formed which deteriorates heat transfer conditions. Direct contact between the surface and liquid is achieved only after the surface temperature decreases below a certain level. The interface between the dry and rewetted surface is called a quench front.[1]

In nuclear reactors, quenching can be observed during the reflood phase of loss-of-coolant accidents (LOCA). Fuel rods are being cooled by the rising steam and the quench front is formed. The quench front is gradually moving upwards and its velocity depends on various parameters such as the surface temperature, flow rate or coolant temperature.

Experimental setup

An experimental loop (Fig. 1) has been designed and built for observing the quenching phenomenon in a vertical channel. The experimental setup consists of a test section with 7 type K thermocouples for measuring the surface temperature, DC power source, heating element with an input power of 1 kW and a capillary for flow rate measurement.

The vertical channel is a 1,2 m long steel tube divided into six sections. It has an inner diameter of 10 mm which roughly corresponds to the flow area between 3 nearest fuel rods in a VVER-1000 reactor. The test section is heated by DC current to a certain initial temperature and continues to be heated throughout the flooding phase to simulate decay heat in a nuclear reactor.

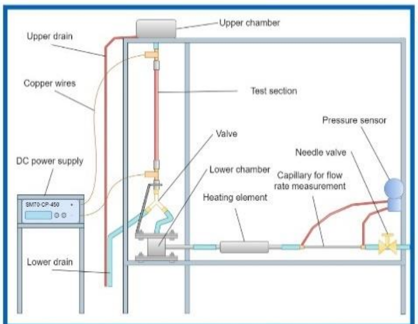

Fig. 1: Schematic of the experimental loop

Initial conditions

The initial conditions were set to be as close as possible to the real situation in a nuclear reactor. The initial wall temperatures ranged from 300 to 750 °C. The coolant mass flow rate was set accordingly to the flow rate during the reflood phase of LOCA, i.e. G = 50 kg/m²s. Since the cooling water in the emergency cooling system tanks is often stored at temperatures below 70 °C, coolant temperatures between 15 and 70 °C were used.[2] The measured data was obtained with a frequency of 100 ms.

Results

Firstly, the progression of the quench front velocity along the height of the test section was observed. It was found that there are two phenomena that have opposite effects on the magnitude of the velocity. The first phenomenon is pre-cooling of the surface by rising steam. When the quench front reaches the upper parts of the test section, the surface temperature is already lower and the quench front can advance faster.

The second phenomenon is the necessity to remove „decay heat“ from the already flooded part of the test section which effectively slows down the progress of the quench front. This effect only becomes apparent at higher initial surface temperatures.

At lower temperatures (up to 400 °C), the pre-cooling outweighs the need to remove heat and the quench front accelerates as it moves upwards in the vertical channel. If we start increasing the initial surface temperature, these two effects begin to balance out and eventually the need to remove „decay heat“ prevails. The comparison of the quench front velocity progression for different initial surface temperatures is shown in Fig. 2.

While these results are valuable, more relevant data can be obtained by calculating the quench front velocity over the entire length of the test section and its dependence on initial parameters. These calculated trends are shown in Fig. 3 and 4.

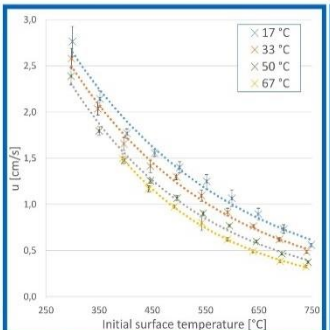

Fig. 3: Quench front velocity for different initial surface temperatures

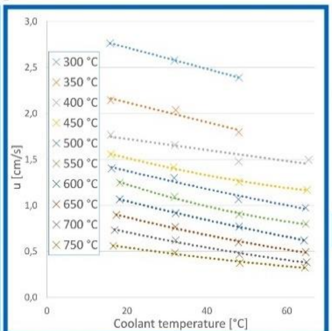

Fig. 4: Quench front velocity for different coolant temperatures

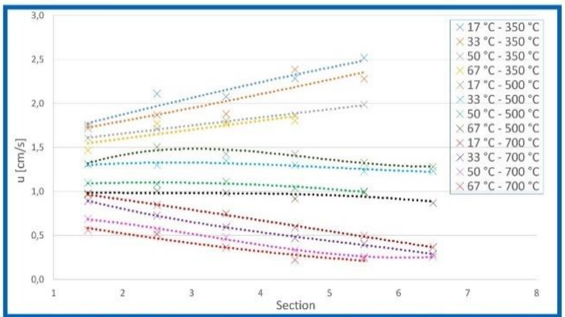

Fig. 2: Quench front velocity progression for 3 initial temperatures

As expected, the quench front moves exponentially faster for lower initial surface temperatures and moves slower for higher coolant temperature used. This linear decrease corresponds to the heat that must be supplied to the quench front to reheat water to saturation temperature, therefore we can conclude that no complex hydrodynamic phenomena occur at higher coolant temperatures.

In addition, the quenching temperatures of each part of the test section were detected. As we can see in Fig. 5, with increasing surface temperature the quenching temperatures deviate more from the linear function due to the aforementioned pre-cooling.

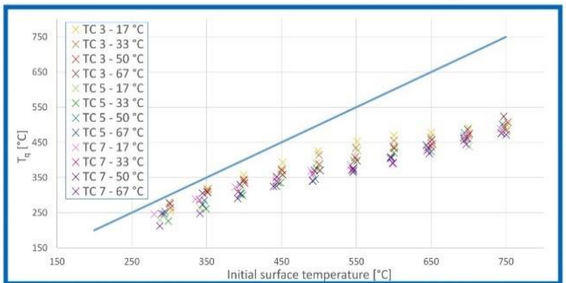

Fig. 5: Quenching temperatures for different surface temperatures

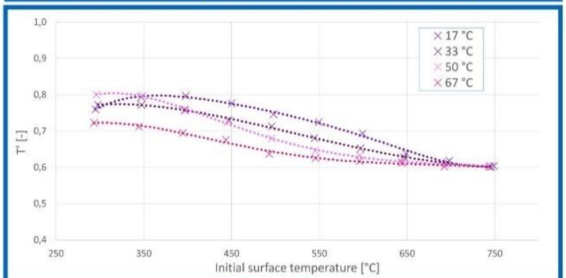

Fig. 6: Relative quenching temperatures

For better comparison relative quenching temperatures were defined and calculated. As we can see in Fig 6, there is a certain temperature above which the solid-liquid contact cannot be established and rewetting is delayed until the temperature drops and the vapour layer near surface collapses.

Conclusion

A set of experiments focused on the quenching phenomenon was conducted. Quench front velocity and its dependence on various initial parameters was calculated and discussed.

References

[1] KIM, Woo Shik; JEON, Byong Guk; JUNG, Satbyoul; KIM, Seok a MOON, Sang-Ki (2022). Optical and thermal visualization of quench front on hot wall during reflood. Annals of Nuclear Energy, 165(108797). ISSN 0306-4549

[2] IWAMURA, Takamichi a ADACHI, Hiromichi (1985). Initial Thermal-Hydraulic Behaviors under Simultaneous ECC Water Injection into Cold Leg and Upper Plenum in a PWR-LOCA. Journal of Nuclear Science and Technology, 22(6), pages 451-460

EXPERIMENTAL VALIDATION OF FLOW HEAT ACCUMULATOR

Jan Loskot

Department of Energy Engineering, Faculty of Mechanical Engineering, Czech Technical University in Prague, Czech Republic

Nuclear fusion could be the greatest energy source if ever contained. Many technical problems have to be solved before its successful realisation and one of them is be the pulsed operation of a tokamak-type reactor which might be resolved with some kind of an accumulation system. The focus of this master's thesis was to develop and experimentally validate a numerical solver for a flow-through solid-state thermal energy storage system. In the future, the developed code might be used for a parametric study of a vast variety of configurations of such an energy storage system.

Experimental validation of flow heat accumulator

Jan Loskot[1,2]

[1]Department of Energy Engineering, Faculty of Mechanical Engineering, CTU in Prague

[2]Department of research and nuclear safety assessment, National Radiation Protection Institute, Prague

CTU CZECH TECHNICAL UNIVERSITY IN PRAGUE

Introduction

The first nuclear fusion power plant (FPP) will most likely use a tokamak-type reactor as its power source. A tokamak generates electric current in the plasma to induce one part of the magnetic field that confines the plasma within the reactor. Electromagnetic induction will most likely be used to generate the electric current in the plasma. Due to physical limitations while using electromagnetic induction, the tokamak will operate in pulsed mode. There will be a “burn” phase followed by a “dwell” phase, lasting 120 and 10 minutes, respectively [1]. One way of compensating for the missing power during the dwell phase is the integration of an energy accumulation system. A solid-state specific heat TES was therefore modeled.

Thesis main goals

1. Develop a numerical solver for a solid-state heat accumulator coupled with simplified HTF model
2. Design and construct an experimental device to provide experimental data for code validation

Thesis results

1. A numerical solver in programming languague *Python* that allows its user to simulate wide range of configurations was developed and tested (Figure 1).
2. An experimental device was designed and constructed. Three measurements were conducted so far and the results were compared to the simulation. Empirical speed correction factors were proposed in order to match the measured data.

An example of simulated accumulator thermal field

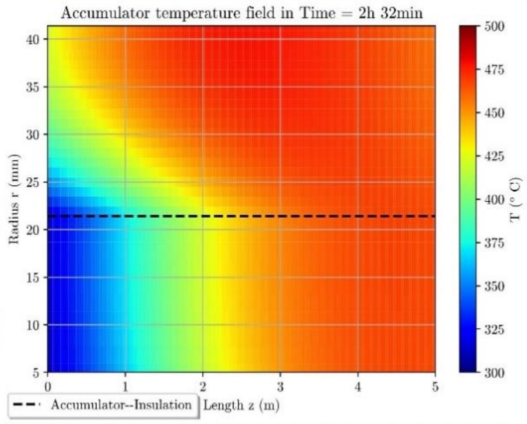

Figure 1: Heat distribution in individual mesh cells of one, insulated, pipe-like element during the beginning of first dwell phase

Panoramatic photo of the designed device

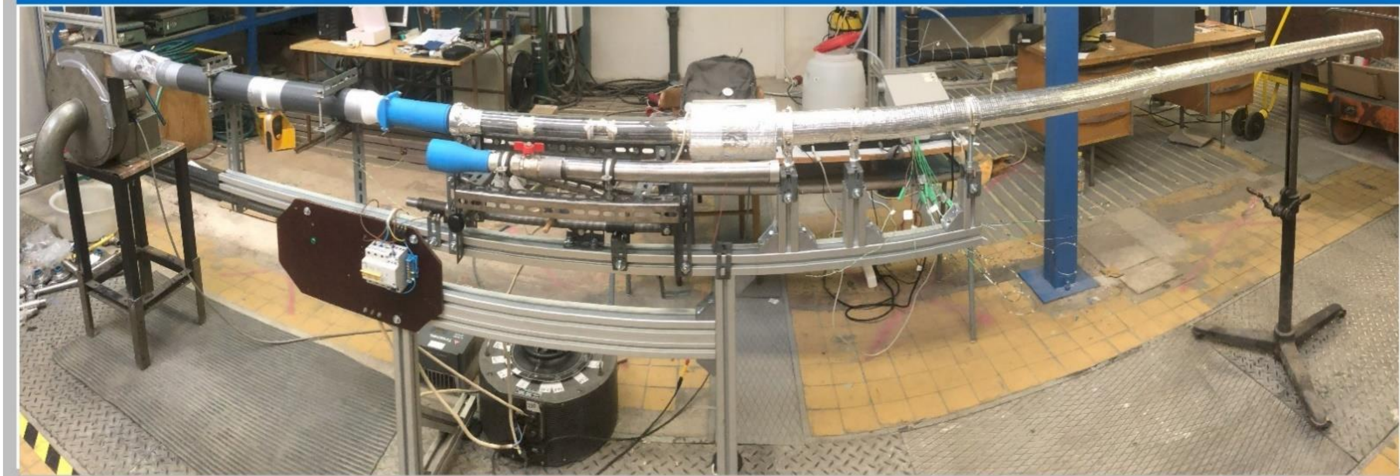

Simulated and measured data comparison

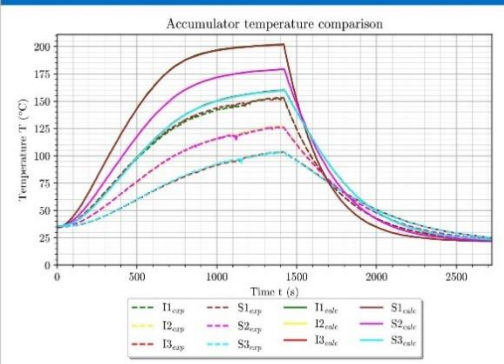

Comparison after speed corrections

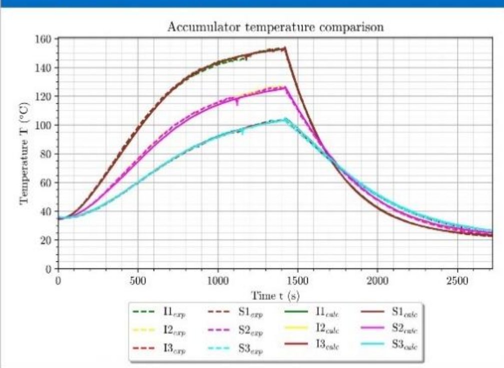

Schematic of the designed device

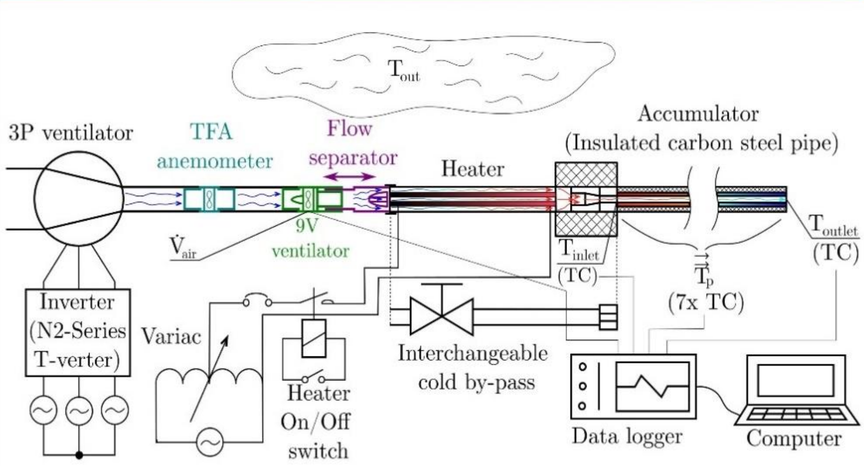

Conclusion

- The device was tested and thermal distribution data of a real accumulator were measured
- The simulated trends were very similar to the measured ones but the absolute values needed corrections
- The code will allow comparison of configurations before doing a detailed study in advanced CFD softwares

References

[1] BARUCCA, L. et al, Maturation of critical technologies for the DEMO balance of plant systems. Fusion Engineering and Design. 2022, vol. 179, p. 113096. Doi: 10.1016/j.fusengdes.2022.113096.

jan.loskot@fs.cvut.cz; jan.loskot@suro.cz

SPENT NUCLEAR FUEL FROM SMALL MODULAR REACTORS

Ondřej Bůžek

Faculty of Electrical Engineering, University of West Bohemia, Czech Republic

This poster focuses on the potential use of SMRs in the Czech Republic, considering the CEZ Group strategy valid at the beginning of 2024. It analyses the SNF (spent nuclear fuel) parameters of potential SMRs and compares them with traditional VVER-1000-type nuclear units. The poster evaluates whether the SNF from SMRs represents a greater burden on the back-end of the fuel cycle compared to the VVER-1000.

FACULTY OF ELECTRICAL ENGINEERING
UNIVERSITY OF WEST BOHEMIA

Spent nuclear fuel from Small Modular Reactors

NUCLEAR DAYS

Ondřej Bůžek [1] Martin Lovecký [2]

[1]buzek@students.zcu.cz [2]lovecky@fel.zcu.cz

Introduction

In the current global energy context, nuclear energy represents one of the promising options for replacing outdated fossil fuel-burning power plants. The most debated topic today are small modular reactors (SMRs), which should fulfill these ambitions. However, although much attention is paid to SMR designs and constructions, the question of spent nuclear fuel (SNF) management needs to be addressed. It is an inherent obligation of any nuclear operator. While most debates focus on the technical and economic aspects of SMR deployments, more attention should be paid to the back-end of the fuel cycle of these reactors.

This poster focuses on the potential use of SMRs in the Czech Republic, considering the CEZ Group strategy valid at the beginning of 2024. It analyses the SNF parameters of potential SMRs and compares them with traditional VVER-1000-type nuclear units. Specifically, it compares decay heat and radiotoxicity of the SNF over a time horizon of one million years. This poster evaluates whether the SNF from SMRs represents a greater burden on the back-end of the fuel cycle compared to the VVER-1000.

Depletion models

Depletion calculations were performed in a computational sequence T-DEPL, which allows the computation of 2D multigroup deterministic transport in NEWT code coupled with ORIGEN code depletion. The library of cross-sections was chosen cross-section library ENDF/B-VII.1 with 252 neutron groups; the latest version 6.2.4.

Table 1. Basic depletion parameters

Reactor	Assembly array	Enrichment (wt%)	Burnup (GWd/t_U)	Specific power (MW/t_U)
VOYGR	17x17 square	4.95	45	26.51
BWRX-300	10×10 square	3.81	49.6	20.05
Rolls-Royce SMR	17x17 square	4.95	60	31.46
NUWARD	17x17 square	4.95	45	27.88
SMART	17x17 square	4.95	54	25.13
SMR-160	17x17 square	4.0	45	19.8
AP300	17x17 square	4.95	62	36.38
Ref. VVER-1000	VVER-1000 hexagonal	4.45	52.8	38.19

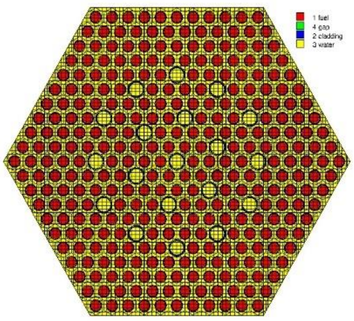

Figure 1. VVER-1000 fuel assembly

Results

The calculated time curves of decay heat in units of W/t_U and radiotoxicity in $m^3{}_{H2O}/t_U$ were normalized during the investigated period. Thus, the results in Figure 2 and 3 are already relative values.

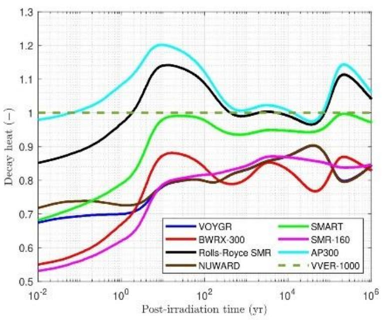

Figure 2. Decay heat normalized by VVER-1000 for projected burnup

In the context of decay heat, SNF from the AP300 and Rolls-Royce SMR reactors represents a greater burden on the back-end of the fuel cycle than SNF from a conventional VVER-1000 reactor. These reactors utilize a higher level of fuel burnup than the reference VVER-1000 reactor. Specifically, SNF from the AP300 results in a 19 % higher burden than fuel from the VVER-1000, while for the Rolls-Royce SMR, this increase is approximately 15 %.

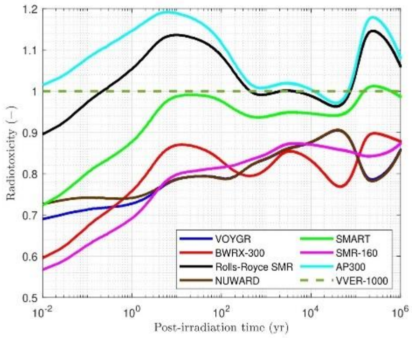

Figure 3. Radiotoxicity normalized by VVER-1000 for projected burnup

Regarding radiotoxicity, it is evident from Figure 3 that SNF from the AP300 and Rolls-Royce SMR reactors will pose a greater burden. Additionally, it is recorded that for the SMART reactor, there was a slight increase in the radiotoxicity of SNF by 1 % around the year 256,000, which is practically comparable to the VVER-1000.

The existing models were adjusted to achieve a comparable burnup of 45 GWd/t_U to eliminate the influence of varying burnup levels. From these results, in the case of comparable burnup, fuels from the examined SMRs will not pose a greater burden on the back-end of the fuel cycle than spent fuel from the VVER-1000.

When assessing the mass of SNF produced per gigawatt of electricity generated annually, it has been determined that fuels with lower burnup levels impose a greater burden on the back-end of the fuel cycle than fuel from the VVER-1000 reactor. Specifically, these fuels include those from the VOYGR, NUWARD, and SMR-160 reactors. Despite slightly higher burnup rates, spent fuel from the SMART reactor also represents a higher burden. Conversely, the best results were achieved by SNF from the BWRX-300, Rolls-Royce SMR, and AP300 reactors.

Table 2. SNF parameters for projected burnup per gigawatt electric-year

Reactor	Decay heat (kW/GW_e-yr) 10th yr	100th yr	Radiotoxicity ($Gm^3{}_{H2O}/GW_e$-yr) 10,000th yr	100,000th yr
VOYGR	40.71 (0.95)	10.37 (0.97)	180.08 (1.07)	14.02 (1.04)
BWRX-300	36.88 (0.86)	8.81 (0.83)	138.57 (0.82)	10.95 (0.81)
Rolls-Royce SMR	39.65 (0.93)	9.42 (0.89)	135.61 (0.81)	11.46 (0.85)
NUWARD	39.94 (0.94)	10.14 (0.95)	176.31 (1.05)	13.69 (1.02)
SMART	44.73 (1.05)	11.12 (1.05)	170.23 (1.01)	13.99 (1.04)
SMR-160	41.47 (0.97)	10.71 (1.01)	180.79 (1.07)	14.12 (1.05)
AP300	41.98 (0.98)	9.76 (0.92)	138.34 (0.82)	11.73 (0.87)
Ref. VVER-1000	42.66 (1.00)	10.63 (1.00)	168.32 (1.00)	13.47 (1.00)

Conclusion

The analysis results show that specific SMRs with higher burnup levels may pose an increased risk in the context of SNF management. These reactors show an increase in decay heat and radiotoxicity up to twenty percent per tonne of initial heavy metal. The results also show that none of the reactors examined at comparable or lower burnup levels show significant increases in decay heat and radiotoxicity requirements.

When considering the mass of SNF generated per gigawatt of electrical production per year, fuels with lower burnup levels pose a greater burden on the back-end of the fuel cycle than reference fuel from the VVER-1000 reactor. Conversely, SNF with higher burnup levels represents a lesser burden.

MODELLING OF NITRIDE SUPERLATTICE COATINGS FOR BWR CLADDINGS

Kamila Oppelová

KTH Royal Institute of Technology, Sweden

Since the Fukushima Daiichi accident, the accident tolerant fuels (ATF) has become a great point of interest. One of ATF's attitudes is to cover the cladding with a thin protective layer of coating. While for PWRs a chromium-metallic coating gives sufficient results, coating material for BWRs is still an object of interest. This poster deals with modelling of (Cr,Nb)N superlattice coating for BWR cladding.

Modelling of nitride superlattice coatings for BWR claddings

Author: Kamila Oppelová[a]

Supervisors: Antoine Claisse[b], Pär Olsson[a]

[a]KTH Royal Institute of Technology, [b] Westinghouse Electric Sweden AB

Introduction and aim

- Zirconium in fuel cladding produces heat and hydrogen when exposed to water/ water steam ⟶ swift reaction at high temperatures ⟶ explosion risk
- After Fukushima accident, development of accident tolerant fuels (ATF)
- 2 attitudes
  - new clad development
  - protective layer of Zr clad ⟶ coating
- Thin layer of metallic Cr is a strong candidate for 1st generation coating for PWRs
- However, the Cr layer dissolves in more oxidising BWR environment
- Results from autoclaves suggest (Cr,Nb)N as a suitable candidate for BWRs coating
- ⟹ AIM: Designing the (Cr,Nb)N coating for BWRs and study the undergoing phenomena

Methods

- Employing density functional theory (DTF) implemented in VASP code
- Rocksalt structure of CrN, NbN, and (Cr,Nb)N is the point of interest
- CrN is modelled as antiferromagnetic
- Comparing of monolithic and superlattice ordering
- The basic cell modelled: 2x2x2 supercell (64 atoms - 16 Cr, 16 Nb, 32 N)
- Superlattices from 1 to 9 atomic layers
- Cr and Nb always in 1:1 ratio

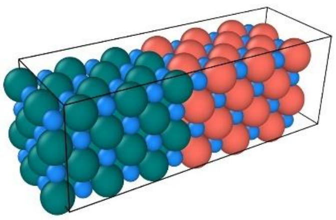

Figure 1: Example of superlattice ordering (6 layers example) visualised by Ovito code [1]

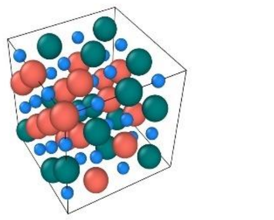

Figure 2: Monolithic mixing (special quasirandom structure - SQS) visualised by [1]

Results

The resulting graph of formation energy as a function of the number of superlattice atomic layers is shown in Figure 3. To better illustrate the trends, the data points in all graphs are connected with dashed lines, although they represent discrete values; these discrete values are marked with "×". Additionally, in Figure 3, the SQS formation energy is included as a constant dotted line for more comprehensive comparison. It is worth noting that the graph features two distinct lines, one for cases with an odd number of atomic layers and the other for an even number. Both lines on the graph are increasing, indicating that the configurations are becoming energetically less favourable as the thickness of the layers increases. Notably, there is a decreasing rate of growth in the formation energy for the odd-numbered layers between layers 7 and 9. Also, as more layers are added, the interfaces created by the boundary conditions affect each other less due to the increasing distance. Eventually, there will be no interaction between these interfaces. With 9 layers, it appears the system is approaching closer to this state. For the even-numbered layers, a similar behaviour can be expected with 10 layers added. However, this could not be verified in the scope of this thesis due to the computational demands required for modelling such geometries.

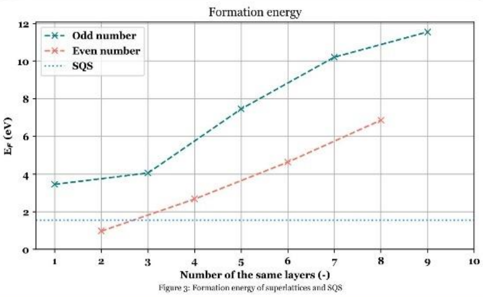

Figure 3: Formation energy of superlattices and SQS

In the superlattice configurations, effect of interfaces on the distance between layers can be observed. It is expected that the thinner the layer, the more prominent the impact of the interface with the boundary case of infinitely thick layers that will have the properties of the bulk material. In Figure 4 and Figure 5 are separately displayed distances among CrN and NbN layers respectively. In both graphs, on x-axis is called "layer gap" indicating between which two layers is the distance corresponds. The numbering takes place from the interface. From the graphs can be seen that CrN and NbN layers thickness quite differently. Unlike CrN layers, the NbN layers are oscillating between two approximately similar values. However, there are some similarities between the graphs. Due to the periodic conditions, the distances remain symmetrical with the symmetry axis in the middle of the layering with odd number of layers creating a plateau.

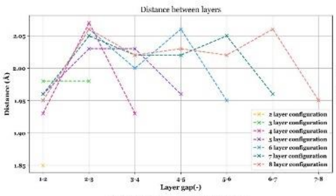

Figure 4: Distance between CrN layers

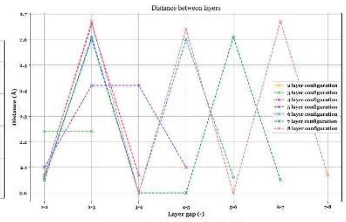

Figure 5: Distance between NbN layers

The shape and behaviour of the distances within the (Cr,Nb)N layers might be explained by the properties of NbN, which forms several lattices with similar formation energies, and the rocksalt structure is not the most stable one. Figure 6 and Figure 7 are used to demonstrate behaviour for even and odd layering. It can be observed that Nb and N atoms do not share the same coordinates in the lattice, which deviates from the rocksalt structure. When a non-cubical cell shape was introduced, the relaxation potential along the cell length increased. The phenomenon observable appears to be NbN attempting to relax to its most stable structure, which is hexagonal. In this hexagonal structure, Nb and N atoms do not share the same plane. These slight shifts explain the fluctuations in the Nb layer distances. When an even number of layers is introduced to the system and the relaxation process begins, there is geometrical space for an ordered sequence of layers, meaning all the layers can relax to their ideal state without disrupting the balance. This results in regular jumps in the total thickness of layers, as demonstrated mainly in coral in Figure 5. When an odd number of layers is introduced, the system still tries to relax as much as possible, but the middle layer becomes the axis of symmetry and lacks the geometrical space for full relaxation. Therefore, this middle layer keeps N and Nb on the same plane, causing a plateau in the thickness between two neighbouring Nb layers, as seen mainly in teal in Figure 5. This issue is also likely the explanation why the trends in Figure 3 needed to be divided into even odd and even layering, since the impossibility of middle layer relaxation results in less stable rocksalt structure layer.

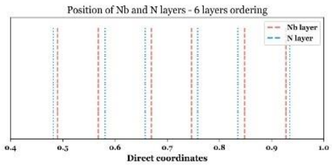

Figure 6: Position of Nb and N layers - even ordering

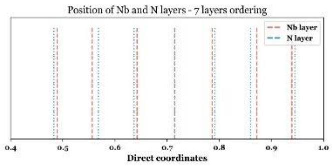

Figure 7: Position of Nb and N layers - odd ordering

Conclusions and future work

- Formation energy increases with number of superlattice layers
- From cases studied, the most stable one is superlattice with 2 layers od CrN and 2 layers of NbN
- Onset of NbN relaxation to its hexagonal lattice was observed
- Non-uniform mixing (different ratios of Cr and Nb)
- Diffusion trough superlattice and SQS
- Detailed effect of oxygen

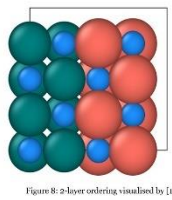

Figure 8: 2-layer ordering visualised by [1]

Also covered in the thesis

- Reference cases - modelling bulk structures and introducing cationic and anionic vacancies; afterwards vacancies were filled with substitational atoms and the effects were studied
- Impact of layering on CrN magnetism and interface thickness
- Oxygen effect on bulk CrN and NbN structures (both in cationic and anionic vacancy, as well as interstitial position)

References

[1] Stukowski, Alexander. "Visualization and analysis of atomistic simulation data with OVITO-the Open Visualization Tool". In: MODELLING AND SIMULATION IN MATERIALS SCIENCE AND ENGINEERING 18.1 (JAN 2010). ISSN: 0965-0393. DOI : {10.1088/0965-0393/18/1/015012}

Fuel rod visualisation: Eloi Pallarès Abril

Download the thesis!

TECHNOECONOMIC ANALYSIS AND OPTIMIZATION OF NUCLEAR MICROREACTORS IN HYBRID ENERGY SYSTEMS BASED ON A DISPATCH STRATEGY

Şevval Fındık

Harbin Engineering University, College of Nuclear Science and Technology, Harbin, China

This poster presents findings from a study on Nuclear Renewable Hybrid Energy Systems (NRHES), evaluating dispatch strategies, comparing with alternatives, and addressing economic uncertainties. Discover insights into system flexibility, reliability, and cost-effectiveness, essential for optimizing NRHES integration into the energy grid.

Technoeconomic Analysis and Optimization of Nuclear Microreactors in Hybrid Energy Systems based on a Dispatch Strategy

AUTHOR

Şevval Fındık

SUPERVISOR

Dr. -Ing. Tian Zhong

AFFILIATIONS

Harbin Engineering University, College of Nuclear Science and Technology

Research drives advancements in energy systems. This poster presents findings from a study on Nuclear Renewable Hybrid Energy Systems (NRHES), evaluating dispatch strategies, comparing with alternatives, and addressing economic uncertainties. Discover insights into system flexibility, reliability, and cost-effectiveness, essential for optimizing NRHES integration into the energy grid.

01. Introduction

NRHES are pivotal in the transition towards sustainable energy solutions, integrating nuclear power with renewables to bolster grid stability amid climate challenges. Despite technical advancements, the economic uncertainties surrounding NRHES configurations remain a critical gap in current research. This study aims to optimize nuclear microreactors within hybrid systems under economic uncertainty, using a blend of real and synthetic data. The primary questions addressed include the performance and economic viability of NRHES configurations, evaluated through metrics such as Net Present Value (NPV), Internal Rate of Return (IRR), and Profitability Index (PI). By leveraging the RAVEN Framework and HERON plugin, this research contributes new insights into the resilience of NRHES to economic fluctuations and its potential to meet future energy demands economically. This study aims to inform policy-makers, industry stakeholders, and researchers on the economic feasibility of integrating nuclear microreactors in hybrid energy systems.

02. Objective

This thesis aims to conduct a comprehensive technoeconomic analysis (TEA) and optimization of NRHES based on dispatch strategy. It focuses on evaluating the operational dynamics and performance indicators of NRHES compared to alternative configurations like natural gas, wind-hydrogen, and solar-wind-hydrogen systems. Key objectives include assessing system flexibility, reliability, and cost-effectiveness, alongside analyzing technoeconomic metrics such as NPV, IRR, and PI. Additionally, the research explores the impact of dispatch strategies on grid security and system reliability, aiming to optimize NRHES integration into the existing energy grid.

Related literature

1. M. A. Arefin, M. T. Islam, F. Rashid, K. Mostakim, N. I. Masuk, and Md. H. Comprehensive Review of Nuclear-Renewable Hybrid Energy Systems: Status, Operation, Configuration, Benefit, and Feasibility', *Frontiers in Sustainable Cities*, vol. 3, Sep. 2021, doi: 10.3389/frsc.2021.723910.
2. Idaho National Laboratory, 'RAVEN'. Accessed: Apr. 16, 2024. [Online]. Available: https://raven.inl.gov/SitePages/Overview.aspx

03. Methodology

A comprehensive review of existing literature was conducted to establish a foundational understanding of NRHES components, their operational characteristics, and integration challenges.

Dispatch Optimization:
- **System Integration:** Integrates microreactors, wind turbines, reversible PEM fuel cell, hydrogen storage, hydrogen market, and grid to meet electricity and hydrogen demands while maximizing NPV.
- **Synergy of Resources:** Combines wind energy's variability with nuclear power's stability for efficient, sustainable energy production.
- **Algorithmic Approach:** Uses dispatch optimization algorithms to maximize hydrogen production during surplus electricity periods and ensure robust hydrogen supply for market and internal use.

Capacity Optimization:
- **Challenges:** Ensures the reversible PEM fuel cell's capacity meets hydrogen market demand constraints to prevent operational inefficiencies.
- **Optimization Algorithms:** Utilizes RAVEN's stochastic gradient descent approach to explore optimization spaces effectively, adjusting step sizes based on gradient directions and performance.

$$M_{opt} = \min_{\vec{C},\vec{D}} \left(\mathbb{E}_\omega \left(M(\vec{C},\vec{D},\omega) \right) \right)$$

Economic Analysis:
- **Capital Costs:** Includes costs for nuclear microreactors, wind turbines, solar panels, PEM fuel cell, and hydrogen storage tanks. Each component's costs are detailed with considerations for installation, integration, and market conditions.
- **Operational Expenses (OPEX):** Accounts for fixed and variable costs related to system maintenance and operation.
- **Allocation Key Method:** Ensures accurate distribution of costs between PEM components (electrolyzer and fuel cell) based on their roles within the system.

Key Assumptions and Parameters: Highlights assumptions guiding the system design, economic evaluations, and financial projections, including stability assumptions for microreactors and natural gas power plants, as well as efficiency values for hydrogen production.
Financial Parameters: Includes inflation rate, discount rate, and tax rate assumptions critical for evaluating project sustainability and financial risks.

To simulate realistic operational scenarios, synthetic histories were generated based on historical weather data, energy demand and price patterns.

04. Results/Findings

The study investigated the feasibility of meeting both 2% and 5% of total electricity demand using three configurations:

- **Configuration 1** (Microreactors, wind turbines, reversible PEM fuel cell, hydrogen storage):
  - Achieved highest economic viability with NPV of $389.2 million and PI of 2.6711 at 2% demand, and NPV of $978.1 million and PI of 6.82 at 5% demand.
- **Configuration 2** (CCGT, wind turbine, reversible PEM fuel cell, hydrogen storage):
  - Showed moderate economic performance, improving to NPV of $80.7 million and PI of 0.9606 at 2% demand, and NPV of $593.2 million and PI of 6.88 at 5% demand.
- **Configuration 3** (Wind turbine, solar panel, reversible PEM fuel cell, hydrogen storage):
  - Demonstrated viability with NPV of $167.4 million and PI of 2.4992 at 2% demand, and NPV of $316.0 million and PI of 4.71 at 5% demand.
- **Uncertainty Analysis**
  - Cost Sensitivity: NRHES exhibited robust economic resilience across varying cost scenarios, maintaining profitability under different cost conditions, particularly under reduced costs.

Synthetic Wind History in Dispatch Window

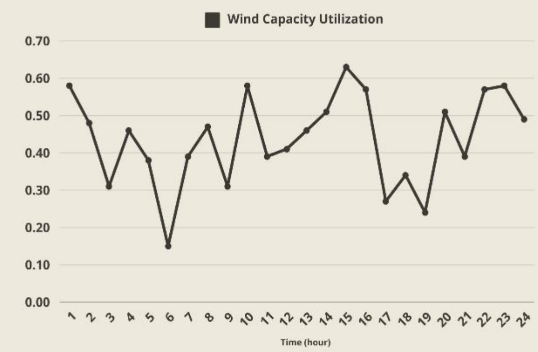

Electricity Dispatch of NRHES

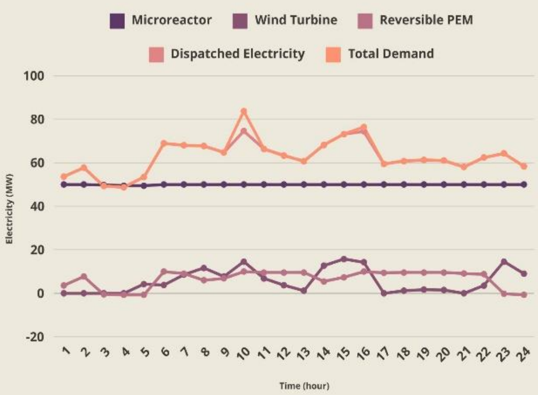

05. Analysis

Strategic Planning for Hybrid Energy Systems
- The study emphasizes that in deregulated markets, aiming to meet 100% of electricity demand at all times may not be cost-effective. Instead, focusing on optimizing economic performance is key, especially during extreme demand scenarios.
- The choice of a lower discount rate significantly enhances economic indicators such as NPV and IRR, making projects more financially attractive. This underscores the importance of selecting an appropriate discount rate in financial assessments.

Comparative Economic Performance of Hybrid Configurations
- Configuration Analysis: Configuration 1 consistently outperformed others in economic viability across both 2% and 5% demand scenarios. Configuration 2 showed potential for profitability with increased demand, while Configuration 3 demonstrated improvement but remained less economically viable.

Sensitivity to Economic Uncertainties
- Impact of Cost Variability: The study's uncertainty analysis highlighted the system's sensitivity to cost fluctuations. Decreases in costs significantly improved economic indicators, whereas increases had adverse effects, underscoring the need for robust financial planning.

Economic indicators of the NRHES under different uncertainties while meeting 5% of total demand

	Percentage of the decrement of the costs			Percentage of the increment of the costs		
	5%	10%	50%	5%	10%.	50%
NPV (billion $)	1.027	1.035	1.103	1.009	1.001	0.933
IRR (%)	42.6	44.6	73.3	39.1	37.6	28.6
PI	7.49	7.79	15.14	6.60	6.24	4.15

Economic Metrics

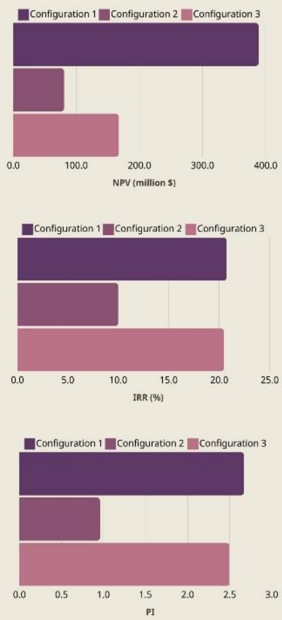

06. Conclusion

This study provides a comprehensive investigation into the analysis and optimization of modern energy systems, offering valuable insights into their design, functionality, and prospects. By meticulously examining various energy sources and system configurations, the research sheds light on critical aspects influencing their performance and economic viability.

Key Findings

- **Integration of Renewable and Conventional Energy:** The study emphasizes the importance of integrating renewable and conventional energy sources in hybrid energy systems. It underscores the need for comprehensive assessments and optimizations to ensure efficiency and sustainability.
- **Superiority of NRHES:** The NRHES emerges as a robust solution, demonstrating superior operational feasibility and economic resilience compared to configurations relying solely on renewable sources.

Implications and Recommendations

- **Sustainability Challenges:** Configurations heavily reliant on conventional energy sources face sustainability challenges, particularly with factors like carbon taxes. Future studies should carefully consider the economic and environmental impacts of traditional energy sources.
- **Future Research Directions:** Future research could explore the impact of varying economic conditions, such as tax rates and discount rates, on energy system performance. Additionally, conducting sensitivity analyses across diverse markets could provide insights into the adaptability and scalability of energy solutions.
- **Enhanced Cost Modeling:** Enhancing cost models to include detailed assessments of hydrogen production and potential market developments can further refine economic evaluations and inform strategic energy planning.

In summary, this study's findings underscore the significance of strategic planning and optimal resource allocation in hybrid energy systems. By integrating stable and renewable energy sources effectively, these systems can achieve a balanced and efficient dispatch mechanism, ensuring reliable and sustainable energy supplies. Future research efforts guided by these insights can contribute to advancing energy system design and operation towards a more sustainable future.

ENHANCING SUSTAINABILITY AND SAFETY FOR A CLEAN ENERGY FUTURE

Emiliia Saprykina

Kharkiv Polytechnic Institute, Kharkiv, Ukraine

This poster explores the multifaceted advancements in nuclear engineering, emphasizing the development of next-generation reactors, waste management techniques, and the pivotal role of nuclear power in combating climate change while ensuring public safety and ecological preservation.

ENHANCING SUSTAINABILITY AND SAFETY FOR A CLEAN ENERGY FUTURE

BY ADVANCING INNOVATIVE REACTOR DESIGNS, IMPROVING FUEL CYCLE TECHNOLOGIES, AND INTEGRATING ROBUST SAFETY PROTOCOLS, NUCLEAR POWER CAN PROVIDE A RELIABLE, EFFICIENT, AND ENVIRONMENTALLY RESPONSIBLE SOLUTION TO MEET THE GROWING ENERGY DEMANDS. THIS THESIS EXPLORES THE MULTIFACETED ADVANCEMENTS IN NUCLEAR ENGINEERING, EMPHASIZING THE DEVELOPMENT OF NEXT-GENERATION REACTORS, WASTE MANAGEMENT TECHNIQUES, AND THE PIVOTAL ROLE OF NUCLEAR POWER IN COMBATING CLIMATE CHANGE WHILE ENSURING PUBLIC SAFETY AND ECOLOGICAL PRESERVATION.

NEXT-GENERATION REACTOR DESIGNS

Focusing on Small Modular Reactors (SMRs) and Generation IV reactors, which offer enhanced safety features, greater efficiency, and reduced waste production.

ADVANCED FUEL CYCLES

Examining closed fuel cycles and the use of thorium, which promise to minimize radioactive waste and improve resource utilization.

ENVIRONMENTAL IMPACT AND SUSTAINABILITY

Assessing the role of nuclear power in reducing greenhouse gas emissions, its minimal land use, and its potential to complement renewable energy sources in a diversified energy portfolio.

PUBLIC PERCEPTION AND POLICY

Addressing the importance of transparent communication, community engagement, and supportive policies to foster public trust and acceptance of nuclear technology.

SAFETY ENHANCEMENTS

Detailing advancements in passive safety systems, real-time monitoring technologies, and rigorous regulatory frameworks that ensure the highest safety standards.

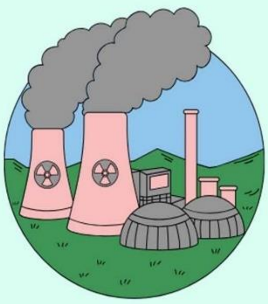

THE INTEGRATION OF THESE ADVANCEMENTS WILL DEMONSTRATE HOW NUCLEAR POWER ENGINEERING CAN BE A CORNERSTONE OF A SUSTAINABLE ENERGY SYSTEM, OFFERING A PATHWAY TO A CLEANER, SAFER, AND MORE SECURE ENERGY FUTURE.

PROSPECTS FOR THE USE OF MODULAR REACTORS IN THE NUCLEAR POWER INDUSTRY OF UKRAINE

Serhii Prokofiev

Odesa National Polytechnic University, Odesa, Ukraine

To determine the advantages of using small modular reactors over VVER-1000 reactors, their designs, safety systems and environmental aspects were compared.

The previous experience of NPP accidents shows that humanity is on the way to improving nuclear facilities aimed at reducing the impact of possible radioactive radiation and radioactive releases on the environment and humanity in general.

Prospects for the use of modular reactors in the nuclear power industry of Ukraine

PUBLIC ATTITUDE

Society has different perceptions of the topic of IMR. It is important to avoid spreading false and biased information, as the public is sensitive to nuclear energy after the Chornobyl accident.

GUARANTEES OF SAFETY AND RELIABILITY

Due to the lack of experience in SMR operation, the guarantee of the declared parameters should be considered a mandatory requirement, regardless of the expert evaluation of the project and the results of its licensing.

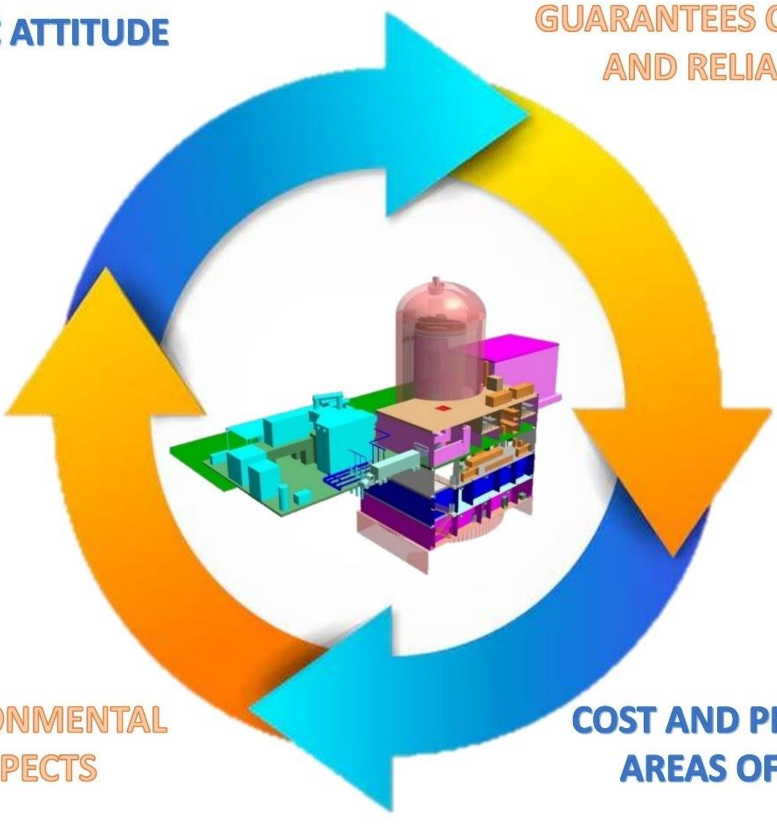

ENVIRONMENTAL ASPECTS

Methodological recommendations should be developed for the preparation of environmental and expert documentation for the IMR (strategic environmental assessment, environmental impact assessment, project for the organization of a sanitary protection zone)

COST AND PRIORITY AREAS OF USE

To date, the issue of the cost of power generation at the MMR has not been fully clarified. It is also necessary to determine the most important directions and ways of implementing SMR, taking into account currentneeds and forecasts of the country's future needs.

Ph.d. STUDENTS

CASE STUDY OF THE FUKUSHIMA NUCLEAR POWER PLANT DISASTER, WHY DID MANAGER YOSHIDA CONTINUE TO INJECT SEAWATER

Yasunobu TAKINAMI

Graduate School of Humanities and Social Sciences, Department of Economics and Management Studies, Saitama University, Japan

The new hypothesis derived from the verification of this case is as follows. An antisocial and inefficient order was issued by the Prime Minister's Office, a higher authority, and TEPCO's head office accepted the order and issued a similar order to the site, but YOSHIDA at the site decided to violate the order and continued to inject seawater. . YOSHIDA's decision to continue injecting seawater suppressed the release of radioactive materials and contributed to ensuring the efficiency of on-site work. In severe accidents, when anti-social and inefficient orders are issued by higher-level agencies, lower-level agencies are required to violate the orders in order to obtain higher value. We present the above new hypothesis.

Case Study of the Fukushima Nuclear Power Plant Disaster
Why did Manager YOSHIDA Continue to Inject Seawater

Yasunobu TAKINAMI

Graduate School of Humanities and Social Sciences, Department of Economics and Management Studies,
Saitama University, 1-7-6 Kanda-Sudacho, Chiyoda-ku, Tokyo 101-0041, Japan
takinami.y.158@ms.saitama-u.ac.jp

Saitama University 埼玉大学

On the afternoon of March 12, 2011, as many experts have pointed out, aggressive seawater injection was necessary. With that in mind, Prime Minister KAN's statements had two main problems.

The first problem with KAN's statement is that it was an anti-social order. There were concerns that if KAN ordered the seawater injection to stop, the nuclear accident would escalate further, increasing the risk that no one would be able to get close to the Fukushima Daiichi nuclear power plant. It can be said that YOSHIDA, who was in command of the scene, had no choice but to violate orders in order to comply with his own social ideas, namely, to ``suppress accidents as much as possible."
The second problem with KAN's comments was that they were inefficient in promoting accident response. At this stage, KAN needed to transfer on-site command authority to YOSHIDA, who had detailed knowledge of the situation, and also issue clear instructions to officials at the Prime Minister's Office to back up seawater injection. As a result, KAN's comments created a conflict of opinion between TAKEGURO and YOSHIDA regarding the injection of seawater, and became a factor that further deteriorated the efficiency of accident handling.
In response to KAN's anti-social and inefficient orders, TEPCO's headquarters accepted KAN's orders and issued instructions to YOSHIDA, the head of the field organization, to stop seawater injection. The mechanism of authority gradient is said to be one reason why lower-level institutions tend to accept orders from higher-level institutions. Milgram's experiment on authority gradients shows the psychological situation of people following the instructions of an authority figure in a closed situation .

Order	Inefficiency	Efficiency
Anti-Social	Anti-Social・Inefficiency Order (Organization Self-destruction Organization Selection)	Anti-Social Order (Organization Selection)
Social	Inefficiency Order (Organization Self-destruction)	Social・Effciency Order (Organization Survival Organization Evolution)

Violation of orders

Violation of orders

Violation of orders

Conclusion
The Independent Investigation Commission on the Fukushima Daiichi Nuclear Accident stated, ``Even if the judgment at the scene was correct after the fact and objectively, there is a serious problem in taking a response that does not follow the orders and instructions of a higher authority. In such a serious situation, it was assessed that the ultimate responsibility rests with the higher-ranking organization, and that lower-ranking organizations should not normally be allowed to take actions that differ from instructions due to their own responsibility. However, we believe that the Fukushima Nuclear Accident Independent Verification Commission's assessment needs to be revised. The new hypothesis derived from the verification of this case is as follows. "

The new hypothesis derived from the verification of this case is as follows. An antisocial and inefficient order was issued by the Prime Minister's Office, a higher authority, and TEPCO's head office accepted the order and issued a similar order to the site, but YOSHIDA at the site decided to violate the order and continued to inject seawater. . YOSHIDA's decision to continue injecting seawater suppressed the release of radioactive materials and contributed to ensuring the efficiency of on-site work. In severe accidents, when anti-social and inefficient orders are issued by higher-level agencies, lower-level agencies are required to violate the orders in order to obtain higher value. We present the above new hypothesis.

Reference: Milgram, S. (1974), Obedience to Authority: An Experimental View, London: Tavistock Publications.
Kensyu KIKUZAWA (2007), "Violating orders will innovate your organization" Kobunsha, Tokyo(Japanese).
House of Representatives (2011), "177th Diet Great East Japan Earthquake Reconstruction Special Committee Minutes No. 6" (https://www.shugiin.go.jp/internet/itdb_kaigirokua.nsf/html/kaigirokua/024217720110531006.htm, (Last confirmed on 2024 April 11th)
Tsuneo FUTAMI (2012), Nuclear power generation accidents/trouble analysis and lessons learned, Maruzen Publishing, pp. 104-105.

Special thanks: For this report, we received partial support for travel expenses from the Atomic Energy Society of Japan.

IN-SITU MOISTURE MEASURING IN CONCRETE STRUCTURES OF CONTAINMENT BUILDING DURING DECOMMISSIONING OF NUCLEAR POWER PLANTS

Tanzila Nurjahan

The poster explores of possible leakage of primary circuit coolant and its impact on containment building. The content of this work is focused on the degradation of concrete structures through cold joints and porous bodies.

In-situ moisture measuring in concrete structures of containment building during decommissioning of nuclear power plants

NUCLEAR DAYS 2024
Student poster competition
12.–13.9.2024

Tanzila Nurjahan[a], Felipe de Assis Dias[b], Eckhard Schleicher[b], Uwe Hampel[a, b]

[a]Chair of Imaging Techniques in Energy and Process Engineering, Technische Universität Dresden, 01062 Dresden, Germany
[b]Institute of Fluid Dynamics, Helmholtz-Zentrum Dresden-Rossendorf, Bautzner Landstraße 400, 01328 Dresden, Germany

Background

During the operation of a nuclear power plant, small amounts of contaminated primary circuit coolant (i.e. water) may leak and penetrate the decontamination coating areas and can propagate into the concrete structures through cold joints and porous bodies.

Objective

Detection of moisture in the containment building
because
moisture is the potential source of contamination.

Moisture sensing process

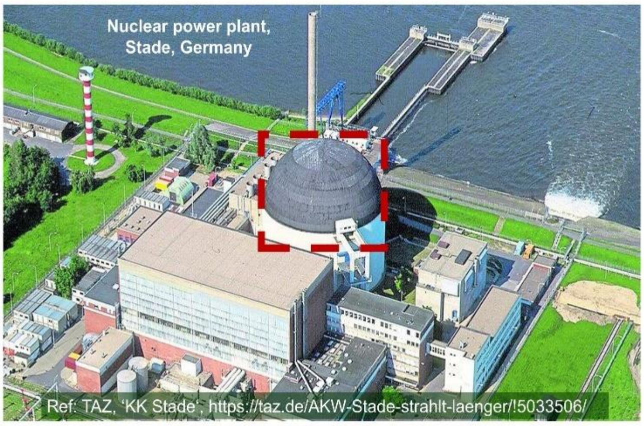

Ref: TAZ, 'KK Stade', https://taz.de/AKW-Stade-strahlt-laenger/!5033506/

Measurement technique

Electrical impedance spectroscopy (EIS)

- Apply sinusoidal voltage and measure the current response

Schematic diagram

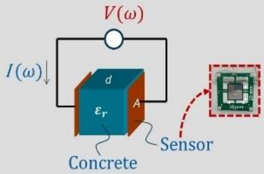

Electrical impedance

$$Z(\omega) = \frac{V(\omega)}{I(\omega)} = \boxed{\frac{-j}{\omega C}}$$

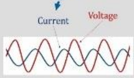

Signal response

Capacitive reactance

- Frequency: 10 Hz - 10 MHz
- Applied signal amplitude: 250 mV

Concrete composition

Concrete sample from **Unterweser nuclear power plant,** Germany

Sensor area

$$\frac{A}{d}\varepsilon_0 \varepsilon_r$$

Sensor distance

Relative permittivity, ε_r of concrete:
- Dry: 4-7 and moist: 8-16
- Moisture sensitive

Porosity, cold joints
- max. 9% of total
- ~ 10 nm..50 µm size

Gravels or stones
- permittivity: 2..8
- ~ 4.5 cm (<) in size

Reinforcement iron
- ~ 2..3% of total
- app. dependent

Results and discussion

Reactance analysis

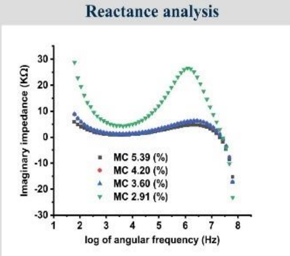

Nyquist diagram

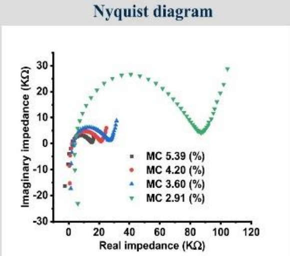

Moisture - impedance

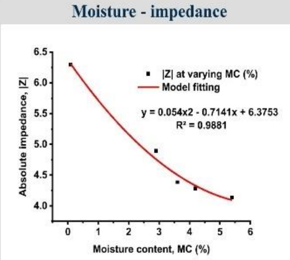

Relative permittivity, ε_r

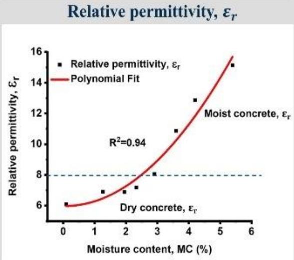

System validation

Parity plot for moisture content, *MC*

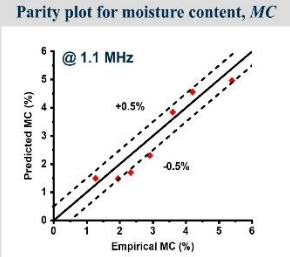

Measurement uncertainty: < ± 0.5%.

Predicted *MC* are in very good agreement with the experimentally obtained *MC*.

Conclusion

Developed system can precisely detect the moisture:

- **Obatined coefficient of determination:**
  - **Relative permittivity, ε_r: 94%**
  - **Moisture content, *MC*: 98%**

The project on which this publication is based is funded by the German Federal Ministry of Education and Research under grant number 15S9434A. The responsibility for the content of this poster lies with the author.

Tanzila Nurjahan
Institut für Energietechnik
Technische Universität Dresden
tanzila.nurjahan@tu-dresden.de,
t.nurjahan@hzdr.de

TECHNISCHE UNIVERSITÄT DRESDEN
HZDR HELMHOLTZ ZENTRUM DRESDEN ROSSENDORF
DRESDEN concept

USING DRONES IN THE NUCLEAR INDUSTRY: INNOVATIONS FOR SAFETY AND EFFICIENCY

Yuliia Hadaieva

Kharkiv Polytechnic Institute, Kharkiv, Ukraine

The integration of unmanned aerial vehicles (UAVs) into the nuclear industry greatly improves the safety and efficiency of facility monitoring. Drones allow for swift data collection in dangerous environments, eliminating the need to jeopardize human lives.

Using Drones in the Nuclear Industry: Innovations for Safety and Efficiency.

Abstract

One of the biggest challenges in the nuclear industry is ensuring the safe and effective monitoring of nuclear facilities.
The IAEA plays a key role in ensuring nuclear safety by developing standards and conducting inspections to guarantee the safe use of nuclear technology for peaceful purposes.

Introduction

Unmanned aerial vehicles (UAVs) and automated radiation control systems (ARCS) are important tools for ensuring safety and monitoring at nuclear facilities. UAVs, unlike traditional ARCS, have several advantages.

Advantages of UAVs:

Rapid Response: UAVs can quickly move to sites of accidents or suspicious objects.
Human Safety: The use of drones allows for data collection without risking human lives.
Accuracy: Drones can be equipped with various sensors and cameras, providing high-precision radiation measurements and detailed inspections of objects.

Development prospects:

1. Use of AI and machine learning for autonomous tasks.
2. Integration with IoT to create a unified monitoring network.
3. Development of drones with increased energy efficiency.

Examples of use:

Fukushima: Drones provided assessments of radiation levels and the condition of facilities after the accident.
Chernobyl: Continuous monitoring of the radiation environment, detection of new sources of contamination, and evaluation of decontamination efforts.

Conclusions

The implementation of unmanned aerial vehicles in the nuclear industry increases the level of nuclear safety, which is critically important for protecting the population and the environment.

Yuliia.Hadaieva@mit.khpi.edu.ua

ANOMALY DETECTION OF MOTOR OPERATED VALVES

Martin Káš, Jindřich Liška

Faculty of Applied Science, University of West Bohemia, Pilsen, Czech Republic

This work focuses on the time domain power analysis for possible nonstandard behavior of motor operated valves. The analysis of signal and preliminary detection of deviation in motor working can mitigate future failure.

DiagEn Laboratory
University of West Bohemia in Pilsen
NTIS European Centre of Excellence
Technicka 8, 306 14, Pilsen, Czechia

FACULTY OF APPLIED SCIENCES
UNIVERSITY
OF WEST BOHEMIA

Anomaly Detection of Motor Operated Valves

Martin Káš, Jindřich Liška

Motivation

- Proper design-based valve and actuator operation is a key factor for the safe and reliably operation of nuclear power plants. According to the World Association of Nuclear Operators, valve issues are the leading cause of forced plant outages.
- Valve repairs can be expensive, especially for contaminated valves, and the availability of long lead time spare parts or obsolete parts can cause difficulties.
- To mitigate the number of valve issues, significant efforts have been undertaken to implement predictive maintenance concepts based on costly and intensive recurrent in-situ testing of the valves and drives.
- In paper [1] author uses a real time torque spectrum estimation for condition monitoring.
- This work focuses on the time domain power analysis for possible nonstandard behaviour [2].

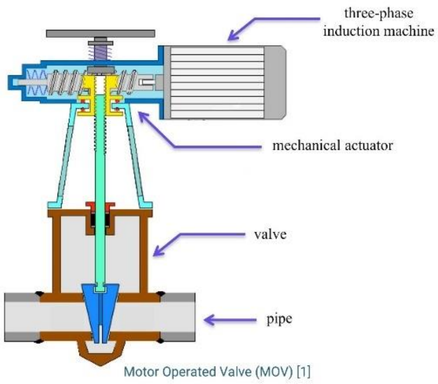

Motor Operated Valve (MOV) [1]

Data Selection

- As input data serves production measurements from different valves since 2018 to 2020. Measurements concerns multiple valves. For data driven analytics tool a sufficient amount of training examples needs to be selected.
- Movement direction of the valve has to be considered for an analysis – whether it is opening or closing.

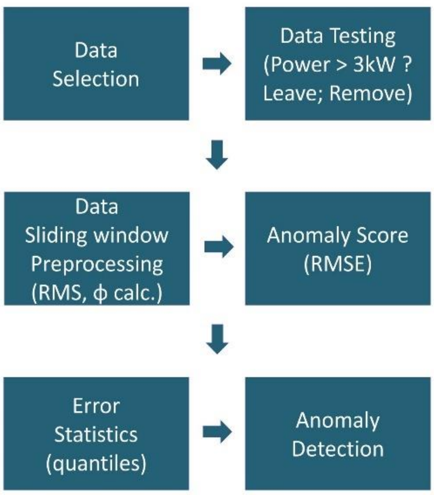

Data preprocessing

- Original sampling rate makes the measurements difficult to analyze. The data also are not consistent in measured characteristics. Some measurements missing a power factor and phase shift. A method of data reduction has been implemented. To prevent excessive information loss a method of sliding window has been chosen. This method calculates from instantaneous values within one period (400 samples in sampling rate of 20 kHz) and effective value of voltages and currents. An overlap of each window is 380 samples - 95%. It also calculates phase shift between voltage and current for calculation of active power. This approach significantly reduces need of computational resources, improves the calculation time but still preserves good response to signal change.

Data Testing

- During the first iteration, it showed up there are some incomplete measurements (missing beginning, missing ending, empty measurements) which corrupts the statistical analysis. The several rules to check the validity of the measurement have to be met - presence of leading power peak and power decrement at the end. If the measurement does not comply these rules, it is excluded from the analysis. The measurement is also trimmed not to have zero values at the beginning and the end.

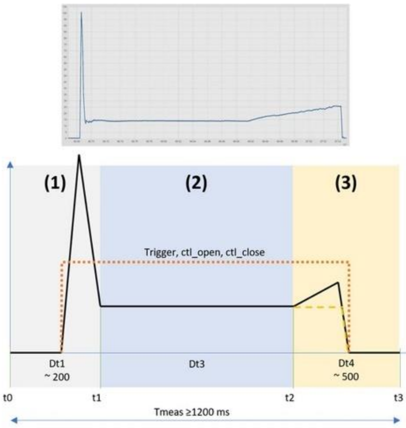

ID	Interval	Duration	Description
1)	T0-T1	~ 200 ms	Starting
2)	T1-T2	~ xxx ms	SteadyState
3)	T2-T3	~ 500 ms	Stopping or StoppingClosing

Movement phases

Anomalies

- Anomalies are data points which deviate from the normal distribution of the whole dataset. These data points need to deviate remarkably from the general distribution of the data. The anomalies form only a very small part of the dataset - up to 2%. These two aspects are fundamental to detecting anomalies.
- Point anomalies: Single data point deviates remarkably from the dataset.
- Collective anomalies: Individual points are not anomalous, but a sequence of these points is anomalous.
- Contextual anomalies: Some data points are normal in a certain situation, while in different situation are detected as anomaly.

Anomaly Score

- Anomaly score in this work is a cumulative value of RMSE of each signals datapoint which steps out of an envelope of the quantile model (5% to 95% quantile).

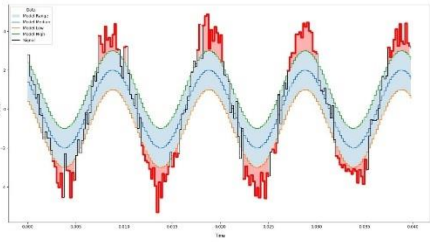

Anomaly Score Principle

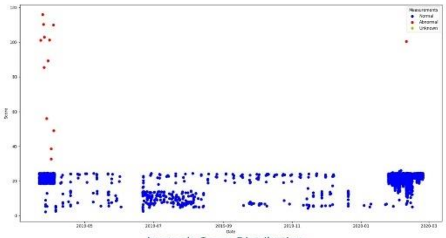

Anomaly Score Distribution

Anomaly detection

- The process of an anomaly detection is based on creating quantile (5%, 50%, 95%) profile of an active power of each measurement. As the measurements vary in length, the model power profile is as long as the longest measurement. When analysing, a particular measurements are compared with just a portion of a model to avoid the unequal length difficulties. For anomaly detection the score is assigned to each measurement. From a data set statistics the anomaly score distribution is calculated. If a particular anomaly score deviates from a distribution significantly, the measurement is marked as an anomaly.

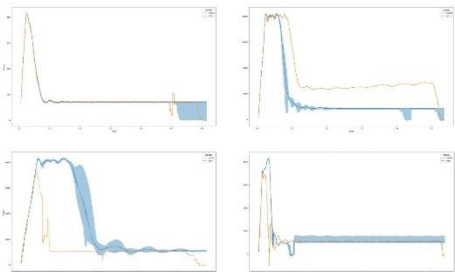

Detected anomalies

Conclusion

- This paper deals with classification of unknown measurements into two classes without any additional information - labels. A statistical algorithm based on root mean square error has been proposed. Shown results represents analysis 78199 measurements in total.
- Two anomaly detection methods were analysed:
  - Statistical approach - quantile based analysis
  - Deep learning approach - autoencoder network
- Statistical approach appeared to be superior in this work with better detection results

References

[1] P. Granjon, "Condition monitoring of motor-operated valves in nuclear power plants",
[2] M. Káš, F. Fomi Wamba, "Anomaly Detection Based Condition Monitoring"

NUCLEAR ENERGY DURING WAR. ENVIRONMENTAL ASPECT

Valeriia Kriuchkova

Kharkiv Polytechnic Institute, Kharkiv, Ukraine

Nuclear power is an integral part of the Ukrainian and global energy sector, even in the face of the growing trend towards the use of alternative energy sources. Despite the fact that this type of energy is a rather complicated and dangerous topic in wartime, a high level of security prevents occupation and terrorist actions from turning a nuclear power plant into an atomic bomb.

NUCLEAR ENERGY DURING WAR. ENVIRONMENTAL ASPECT

NUCLEAR POWER IN THE WORLD

416 reactors
The total capacity is
374671 MW

59 reactors
with a total capacity of
61647 MW
are under construction

25 reactors
are under construction.
The total capacity of
21272 MW
is suspended

210 reactors
Total capacity of
106020 MW
decommissioned

ADVANTAGES AND DISADVANTAGES

- Nuclear power plants are used to generate almost a third of the world's carbon-free electricity
- Nuclear’s fuel calorifsc value 2 million times ↑ than oil ↑ than coal

- Danger of nuclear accidents
- High construction and operation costs compared to alternative energy sources
- Problems with increased radiation levels and waste disposal
- Potential risk to create nuclear "dirty bomb" using nuclear`s power plant technologies and resource

NUCLEAR ENERGY DURING MILITARY CONFLICT

- A stable source of electricity in the face of the destruction of critical infrastructure
- Practical independence from fuel sources
- Unlike alternative energy sources, the energy sector is resistant to missile attacks
- No destroyed nuclear power plants-no needs for urgent waste disposal. For example, buttery & accumulators from solar panels are hazardous and after missile attack and destruction mast be dispose with special conditions

- Occupation. On 4 March 2022, Europe's largest nuclear power plant with a capacity of 6,000 MW (Zaporizhzhia NPP) was occupied by the Russian military.
- Radiation released into the environment as a result of shelling
- Secondary contamination. Fire and landscape changes in the Chernobyl NPP exclusion zone as a result of increased contamination

CONCLUSION

- Nuclear energy is an indispensable part of the Ukrainian and global energy sector, even taking into account the increase in the use of alternative energy sources
- High level of security prevents occupation and terrorist actions from turning NPPs into atomic bombs
- The safety of nuclear power depends on the human factor
- Nuclear energy should be used only for peaceful purposes

Valeriia.Kriuchkova@mit.khpi.edu.ua

NUCLEAR DAYS 2024
STUDENT POSTERS

Editor: Jan Zdebor

Published by:
University of West Bohemia,
Univerzitní 2732/8, 301 00 Pilsen, Czech Republic

1st edition, 49 pages
Pilsen 2024

ISBN 978-80-261-1243-3